



National Library
of Canada

Bibliothèque nationale
du Canada

Canadian Theses Service

Service des thèses canadiennes

Ottawa, Canada
K1A 0N4

NOTICE

The quality of this microform is heavily dependent upon the quality of the original thesis submitted for microfilming. Every effort has been made to ensure the highest quality of reproduction possible.

If pages are missing, contact the university which granted the degree.

Some pages may have indistinct print especially if the original pages were typed with a poor typewriter ribbon or if the university sent us an inferior photocopy.

Reproduction in full or in part of this microform is governed by the Canadian Copyright Act, R.S.C. 1970, c. C-30, and subsequent amendments.

AVIS

La qualité de cette microforme dépend grandement de la qualité de la thèse soumise au microfilmage. Nous avons tout fait pour assurer une qualité supérieure de reproduction.

S'il manque des pages, veuillez communiquer avec l'université qui a conféré le grade.

La qualité d'impression de certaines pages peut laisser à désirer, surtout si les pages originales ont été dactylographiées à l'aide d'un ruban usé ou si l'université nous a fait parvenir une photocopie de qualité inférieure.

La reproduction, même partielle, de cette microforme est soumise à la Loi canadienne sur le droit d'auteur, SRC 1970, c. C-30, et ses amendements subséquents.

UNIVERSITY OF ALBERTA

**WEATHERING, TRACE ELEMENTS, AND SMECTITE STABILITY
IN EXTREMELY ACID SOIL ENVIRONMENTS.**

BY

CARL JAMES WARREN



A thesis submitted to the Faculty of Graduate Studies and Research in partial fulfillment
of the requirements for the degree of

DOCTOR OF PHILOSOPHY

IN

SOIL CHEMISTRY

DEPARTMENT OF SOIL SCIENCE

EDMONTON, ALBERTA

FALL, 1991



National Library
of Canada

Bibliothèque nationale
du Canada

Canadian Theses Service Service des thèses canadiennes

Ottawa, Canada
K1A 0N4

The author has granted an irrevocable non-exclusive licence allowing the National Library of Canada to reproduce, loan, distribute or sell copies of his/her thesis by any means and in any form or format, making this thesis available to interested persons.

The author retains ownership of the copyright in his/her thesis. Neither the thesis nor substantial extracts from it may be printed or otherwise reproduced without his/her permission.

L'auteur a accordé une licence irrévocable et non exclusive permettant à la Bibliothèque nationale du Canada de reproduire, prêter, distribuer ou vendre des copies de sa thèse de quelque manière et sous quelque forme que ce soit pour mettre des exemplaires de cette thèse à la disposition des personnes intéressées.

L'auteur conserve la propriété du droit d'auteur qui protège sa thèse. Ni la thèse ni des extraits substantiels de celle-ci ne doivent être imprimés ou autrement reproduits sans son autorisation.

ISBN 0-315-70000-9

Canada

UNIVERSITY OF ALBERTA

RELEASE FORM

NAME OF AUTHOR: Carl James Warren


TITLE OF THESIS: Weathering, trace elements, and smectite stability
in extremely acid soil environments.

DEGREE: Doctor of Philosophy

YEAR THIS DEGREE GRANTED: 1991

Permission is hereby granted to the University of Alberta Library to reproduce single copies of this thesis and to lend or sell such copies for private, scholarly or scientific research purposes only.

The author reserves other publication rights, and neither the thesis nor extensive extracts from it may be printed or otherwise reproduced without the author's written permission.


.....
(Student's signature)

Permanent address:

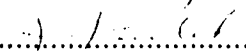
12-180 Marksam Road
Guelph, Ontario, Canada
N1H 8G6

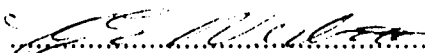
Date: September 9, 1991

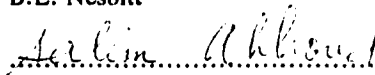
UNIVERSITY OF ALBERTA
FACULTY OF GRADUATE STUDIES AND RESEARCH

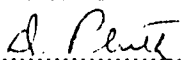
The undersigned certify that they have read, and recommend to the Faculty of Graduate Studies and Research, for acceptance, a thesis entitled WEATHERING, TRACE ELEMENTS, AND SMECTITE STABILITY IN EXTREMELY ACID SOIL ENVIRONMENTS submitted by CARL JAMES WARREN in partial fulfillment of the requirements for the degree of DOCTOR OF PHILOSOPHY in SOIL CHEMISTRY.

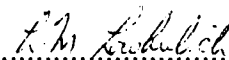

M.J. Dudas (Supervisor)


S. Pawluk


B.E. Nesbitt


S.A. Abboud


D.J. Pluth


L.M. Lavkulich (External)

Date: September 9, 1991

To Vicki

ABSTRACT

The extremely acidic environment developed in what was initially calcareous till located beside a 25 year old elemental sulfur block was used to study the effects of acidity on the weathering of soil minerals, the redistribution of inherent trace elements, and on the chemical composition, layer charge density, and stability of soil smectite. The pH value of the surface material was 2.1. The underlying non-acidified till remained calcareous with pH values of 7.8 and was separated from the acidified material by an Fe-enriched, indurated layer 10 to 15 cm thick. Iron dissolved primarily from Fe-rich primary minerals in the acidified material reprecipitated to form the layer in response to the increased pH environment with depth. The layer emerged at the surface about 3 m from the block and dipped under the block at an angle of 27°. Calcium derived primarily from carbonate was precipitated as gypsum in the acidified material. Iron-containing primary minerals, chlorite, smectite, and plagioclase feldspars were partially or completely dissolved in the acidified material. Arsenic, Co, Ga, Mn, Sc, Th, U, Zn, and the lanthanide elements were depleted in the surface relative to the calcareous material. Arsenic, Co, and Ga were enriched in the indurated layer. Pore water extracted from the acidified material contained high concentrations of SO_4^{2-} , Al, and Fe. Smectite in the calcareous material was identified as montmorillonite with a calculated half-cell formula of $\text{M}^{+0.40}(\text{Si}_{3.96}\text{Al}_{0.04})(\text{Al}_{1.56}\text{Fe}^{3+0.10}\text{Mg}_{0.33})\text{O}_{10}(\text{OH})_2$. Smectite remaining in the acid material had a formula of $\text{M}^{+0.34}(\text{Si}_{3.98}\text{Al}_{0.02})(\text{Al}_{1.66}\text{Fe}^{3+0.10}\text{Mg}_{0.16})\text{O}_{9.92}(\text{OH})_{2.08}$ indicating incongruent dissolution with a decrease in layer charge density and preferential loss of octahedral Mg. Values for ΔG°_f and $\text{Log } K_{eq}$ were derived mathematically from the chemical compositions. All smectites were predicted stable in the calcareous material, but not stable in the acidic material. Simulated increases in the amount of tetrahedral replacement of Al for Si or decreases in the content of octahedral Fe predicted a reduction in the stability of the smectite with respect to the chemistry of the pore water in the acidified material. Chemical weathering of the smectite resulted in evolution of the structural composition towards that of pyrophyllite and did not favour formation of tetrahedrally substituted structures.

ACKNOWLEDGEMENTS

I would first like to thank the various institutions and trusts responsible for financial support of this project. The bulk of the research was supported by the Natural Sciences and Engineering Research Council of Canada through grants to Dr. M.J. Dudas. Support in the form of awards and scholarships was provided by the Canadian Environmental Assessment Research Council, the Province of Alberta, the Alberta Sugar Company and, most notably, the Izaak Walton Killam Memorial Trust of the University of Alberta. I also thank Amerada Minerals of Canada Ltd. for allowing access to the field site.

I am indebted to a large number individuals who guided my progress towards the completion of this document. First and foremost is my supervisor, Dr. Marv Dudas, who provided encouragement, support, and a great deal of his valuable time for enumerable discussions that always seemed to benefit me far more than him. I also thank Drs. S. Pawluk, B.E. Nesbitt, S.A. Abboud, D.J. Pluth, and L.M. Lavkulich for wading through these pages, making valuable suggestions, and generally serving on the examining committee. Thanks are also due to the faculty members who faithfully served on my other various examination committees, dreamed up questions to prod my intelligence, and put up with my numerous queries. Gentlemen, your patience is commended and will long be remembered and appreciated. Special thanks are also extended to Dr. D.A. Laird, Department of Agronomy, Iowa State University, and to Prof. Dr. G. Lagaly, Institut für anorganische Chemie der Universität Kiel, Kiel, Germany for their communications regarding the alkylammonium procedure.

Finally, I would be very much amiss if I did not also give honorable mention to those many highly talented individuals with whom I shared the laboratory. Their contributions to the content of this document, if not from their words, were derived from their actions. Those deserving of most honorable mention are Mr. Micheal Abley, Dr. (about time) Graeme A. Spires, Dr. David L. Burton, Ms. Laura Toerper and numerous other FOP members the list of which would likely fill another page. My education would have been far less rounded without the usual frank exchange of ideas related to the problems of the day, or discussions on the newest developments in computerware. The running games of chess with Mikey were always a welcome challenge and diversion to help maintain my sanity.

TABLE OF CONTENTS

CHAPTER	PAGE
1. Introduction	1
1.1 References	5
2. Acidification adjacent to an elemental sulfur stockpile:	
I Mineral weathering	9
2.1 Introduction	9
2.2 Materials and Methods	10
2.3 Results and Discussion	13
2.3.1 Profile Characteristics	13
2.3.2 Primary Minerals	20
2.3.3 Clay Minerals	23
2.4 Conclusions	28
2.5 References	29
3. Acidification adjacent to an elemental sulfur stockpile:	
II Trace element redistribution	32
3.1 Introduction	32
3.2 Materials and Methods	33
3.3 Results	34
3.4 Discussion	38
3.5 References	42

4.	Dynamics of soil solution chemistry during laboratory incubation of soil samples at 25°C	44
4.1	Introduction	44
4.2	Materials and Methods	47
4.3	Results and Discussion	49
4.4	Conclusions	64
4.5	References	65
5.	Layer charge density and chemical composition of smectite in a western Canadian soil	68
5.1	Introduction	68
5.2	Materials and Methods	69
5.3	Results and Discussion	71
5.3.1	Layer Charge Density	71
5.3.2	Chemical Composition	78
5.4	Conclusions	86
5.5	References	87
6.	Free energy of formation of a soil smectite and predicted stability in an extremely acidic soil	91
6.1	Introduction	91
6.2	Materials and Methods	92
6.3	Results	95
6.4	Discussion	106
6.5	Conclusions	109

6.6	References	111
7.	GENERAL DISCUSSION AND CONCLUSIONS	114
7.1	References	118
APPENDIX.	Simple microwave digestion technique for elemental analysis of mineral soil samples	121
A.1	Introduction	121
A.2	Materials and Methods	122
A.3	Results	123
A.4	Discussion	124
A.5	References	125

LIST OF TABLES

Table 2.1	Description and some chemical properties of soil samples at 5 cm depth increments representative of the profile exposed at a distance of two meters from the edge of the sulfur block	14
Table 2.2	Chemical composition of bulk soil samples from selected depths in the profile at a distance of two meters from the edge of the sulfur block	18
Table 2.3	Mean concentrations ($\text{g}\cdot\text{kg}^{-1}$) of Fe, Al, and Si extracted from selected samples by Na-pyrophosphate, acid ammonium oxalate, and citrate-bicarbonate-dithionite methods	19
Table 2.4	Mean mineralogical composition of the sand fraction from selected depths in the profile	22
Table 2.5	Some physical and chemical characteristics, qualitative estimates of kaolinite, and semi-qualitative estimates of chlorite in the total clay separates from selected depths	24
Table 3.1	Concentration of trace elements in bulk samples from selected depths in the profile	36
Table 3.2	Concentration of lanthanides in the bulk samples from selected depths in the profile	37
Table 4.1	Percent distribution of components among aqueous species in the extracts from the air dried and non-dried acidic samples after 1 day and 128 days of incubation	58
Table 4.2	Percent distribution of components among aqueous species in the extracts from the air dried and non-dried calcareous samples after 1 day and 128 days of incubation	59
Table 4.3	Saturation indices for selected primary and secondary minerals calculated with respect to the extracted soil solutions after 128 days of incubation	61

Table 5.1	Mean values (n=3) chemical compositions (g·kg⁻¹) for the bulk clay and the calculated composition of smectite from the 0 to 10 cm (acidic) depth and the 55 to 75 cm (calcareous) depth	79
Table 5.2	Unit half-cell formulas and quantities (g·kg⁻¹) of minerals and amorphous phases in the < 2 µm size fraction separated from the acidic and calcareous layers	80
Table 6.1	Total concentrations and calculated distribution among species for the major elemental components in the soil solutions extracted after incubation of the samples from the 0 - 10 cm depth	96
Table 6.2	Total concentrations and calculated distribution among species for the major elemental components in the soil solutions extracted after incubation of the samples from the 35 - 45 cm depth	97
Table 6.3	Total concentrations and calculated distribution among species for the major elemental components in the soil solutions extracted after incubation of the samples from the 45 - 50 cm depth	98
Table 6.4	Total concentrations and calculated distribution among species for the major elemental components in the soil solutions extracted after incubation of the samples from the 65 - 80 cm depth	99
Table 6.5	Comparison of predicted stability and observed presence of selected primary and secondary minerals	102
Table 6.6	Chemical composition and calculated free energy of formation values (kJ·mol⁻¹) for smectites with Mg, Al and Ca on the exchange sites	103
Table A.1	Recommended values mean (n=8) analytical values, with 95% confidence limits, and relative standard deviations (RSD) for four reference soil samples	124

LIST OF FIGURES

Figure 2.1	Schematic three dimensional diagram of the sample site indicating the position and orientation of the sample pits with respect to the elemental sulfur block and a cut away section displaying the orientation of the sampled materials and layers	16
Figure 2.2	X-ray diffractograms obtained for Ca-saturated and K-saturated clay specimens from the acidified (0 to 5 cm depth) and calcareous parent till obtained 50 m from the block	25
Figure 4.1	Moisture retention curves for the acidic and calcareous soil samples	51
Figure 4.2	Measured pH values (with standard deviations) of pore water extracted from the acidified and calcareous samples plotted against number of days after the start of incubation	52
Figure 4.3	Total concentrations (with standard deviations) of Al, Si, Fe, and Ca in the pore waters samples extracted from the air dried and non-dried acidified and calcareous samples plotted against number of days after the start of incubation	54
Figure 4.4	Total concentrations (with standard deviations) of K, Mg, P, and SO ₄ in the pore waters samples extracted from the air dried and non-dried acidified and calcareous samples plotted against number of days after the start of incubation	55
Figure 4.5	Saturation indices for jurbanite and gypsum in the acidic sample and gypsum and calcite in the calcareous sample plotted against number of days after the start of incubation	63
Figure 5.1	X-ray diffraction patterns for the alkylammonium saturated clay separates from the acidified material	72
Figure 5.2	Relationship between basal spacing (d-spacing) and length of alkylammonium carbon chain for clay sized separates from the acidified layer and the calcareous layer displaying a monolayer-bilayer transition	74

Figure 5.3	Relationship between basal spacing (d-spacing) and length of alkylammonium carbon chain for clay sized separates from the acidified layer and the calcareous layer displaying formation of a paraffin-like structure in the interlayer	75
Figure 5.4	Histograms for the distribution of layer charge densities (σ) for smectite from the acidic and calcareous materials	77
Figure 6.1	Saturation indices (SI) for the soil solution extracts from the four layers calculated with respect to selected primary and secondary minerals	100
Figure 6.2	Saturation indices (SI) for Al- and Ca-saturated smectites calculated with respect to the chemical compositions of the soil solution extracts from the four selected layers	105

1. INTRODUCTION

Acidification is a natural process that occurs in all soils. Most virgin soils in temperate regions reflect the pH values of meteoric waters which are naturally acidic (theoretical $\text{pH} = 5.6$) due to absorption of atmospheric CO_2 . Modern industrial and agricultural activities have increased the amount of acid forming materials intercepted by soils. Emissions of acid forming gaseous oxides of sulfur and nitrogen from industrial facilities have drastically decreased the pH levels of precipitation in some areas resulting in the phenomenon known as acid precipitation (Coburn and Likens 1974). On agricultural soils, acidity derived from applied fertilizers greatly exceeds acidic inputs from atmospheric sources (Hofstra 1986). Over the past 25 years, rapid declines in soil pH values have been observed in some cultivated soils (Mahler et al. 1985). Ammonium containing fertilizers are the most notorious acidifiers. Long term application has been shown to significantly reduce soil pH values (Berg 1986) and reaction of fertilizer placed in concentrated bands can temporarily generate extremely acidic conditions within localized zones in soil. Elemental sulfur is yet another acid forming material. Oxidation of elemental sulfur in soil can result in decreases in soil pH values proportional to the applied amount (Nor and Tabatabai 1977). In some instances acidification can be severe. For example, elemental sulfur dust escaping from stock piles at natural gas desulfurization facilities has been known to acidify localized areas of land downwind of the source to pH values less than 2.0 (Nyborg 1978).

Extreme acidity can also develop naturally in some soils. Such soils include acid sulfate soils which are naturally occurring soils that generally exhibit pH values in the extremely acid range ($\text{pH} < 4.5$). Acid sulfate soils usually develop in parent materials that contain significant quantities of sulfide minerals: most commonly pyrite (FeS_2). The most common parent materials are marine shales and artificially drained tidal flats. The extreme acidity is developed as a result of the rapid oxidation of sulfide minerals to form of H_2SO_4 (Nordstrom, 1982; Lietze and Peterson, 1987).

The level of hydrogen ion activity plays an important role in almost all chemical reactions that occur in soils. Among the most important are the reactions controlling the stability and exchange

reactions of soil clay minerals. The abundance and types of clays in mineral soils dictate the ability of the soil to retain nutrients and maintain fertility levels. Some examples of how hydrogen ion activity (level of acidity) influences the chemistry of soil clay minerals include: substitution into exchange reactions and shifting equilibria; protonation or deprotonation of charge sites dictating pH dependent charge; and stabilization or destabilization of clay mineral structures by shifting the mass balance for mineral stability reactions and/or the speciation of dissolved elemental components.

Smectites are responsible for a large percentage of the exchange capacity of soils of the Interior Plains region of western Canada. Smectites alone or smectites plus illitic clays are commonly reported to constitute greater than 50% of the clay mineral suites of soils on the Canadian prairies (St. Arnaud and Mortland 1963; Brunelle et al. 1976; Kodama 1979; Abder-Rahman 1980; Dudas and Pawluk 1982; Badraoui et al. 1987). The inherently high exchange capacity of smectite is responsible for the mineral being an important source of exchange capacity in these soils.

Based on thermodynamic calculations, smectites are predicted to be unstable under most conditions in acidic soil environments. Hydrogen ion activity is the single most important variable in determining the stability of smectite in soil systems (Kittrick 1971). Montmorillonite is usually undersaturated in acidic solutions in the presence of kaolinite and amorphous silica, but it may be stable if the concentrations of Si and Mg in solution are maintained at high levels (Kittrick 1971; Weaver et al. 1971; 1976; Karathanasis and Hajek 1984). High concentrations of Si in solution are usually maintained at the expense of primary soil minerals (Kittrick 1969).

Based on the above mentioned theoretical predictions, one would intuitively expect to find smectites absent or in the process of decomposing in soils subjected to strong acidity. Carson and coworkers (1976) suggested that smectite dissolution in acidic soils occurs congruently with little loss of exchange capacity. Other investigators have suggested that some smectites may be stable or even forming in some acidic soil horizons. Smectite has been identified as one of the dominant clay minerals among the clay sized fractions of some acid sulfate soils in western Canada (Pawluk 1971; Curtin and Mermut 1985). In other instances they are reported to be absent or constitute only a minor component (Clark and Green 1964; Pawluk and Dudas 1978; Bulmer 1987). Douglas (1982) identified beidellitic

smectite clays among the clay mineral suite of three highly acidic ($\text{pH} < 4.5$) Podzolic soils of New Jersey. Ross and Mortland (1973) had previously postulated that beidellite forms in acidified soil profiles during the alteration of clay sized micas and vermiculite phases. Based on increased concentrations of beidellite in the coarse clay fraction ($2 - 0.2 \mu\text{m}$), Badraoui and coworkers (1987) similarly suggested that beidellite forms in acidic soils by the weathering of micas through vermiculite intermediates. Inherited montmorillonite in such soils may decompose as beidellite forms from micas (Senkayi et al. 1985). Robert (1973) suggested that the amount of tetrahedral substitution in the parent mica dictates whether the weathering product is vermiculite or smectite.

Other theoretical calculations and mineralogical observations support the suggestion that beidellite smectite is stable in acidic soils. Beidellite is observed as a minor phase along with an abundance of montmorillonite in the clay sized fractions of Alberta soils (Dudas and Pawluk 1982). Thermodynamic calculations suggest that beidellite, the Al-rich end member of the smectite solid solution series, is favoured for reactions involving incongruent dissolution between montmorillonite and beidellite (Merino and Ransom, 1982; Karathanasis and Hajek 1983). Wide ranges in heterogeneity of charge density in individual montmorillonite clay particles also suggest that incongruent dissolution to form beidellite and vermiculite is possible (Machajdik and Cicel 1981; Talibudeen and Goulding 1983). Consistent with the presence of beidellite in acidic soils are the many laboratory experiments dealing with the dissolution kinetics of smectites in acidic solution. Such experiments demonstrate that the octahedral layers of 2:1 phyllosilicates dissolve more rapidly than tetrahedral layers (Mathers et al. 1955; Osthau 1954; 1956; Carrol and Starkey 1971; Novak and Cicel 1978). Grim (1968) indicates that 75 to 85% of the total Al in montmorillonite structures can be removed before the structure disintegrates. In contrast, Sridhar and Jackson (1974) and Churchman and Jackson (1976) argue that dissolution of smectites is incongruent with a greater proportion of Al dissolved from the mineral leaving a Si rich end member. This argument implies that the amount of tetrahedral substitution of Al for Si decreases as dissolution progresses under acidic conditions.

In addition to the crystallochemical composition of clay minerals, the nature of the cations on the exchange sites may also influence mineral stability (Kittrick 1979). Both structural Mg and Al

replace H^+ on the exchange sites of smectites in acidic environments (Barshad 1960a; 1960b; Coleman and Craig 1961; Barshad and Foscolos 1970; Frenkel et al. 1983). Pawluk (1961) suggests that exchangeable Al stabilizes smectite in acidic soils. It is apparent that the magnitude of the effect of the type of cation on the exchange site is small relative to the total composition of the clay, but the effect must still be considered (Mattigod and Sposito 1978).

The observations listed above suggest that montmorillonite may or may not be stable in extremely acidic soils and that beidellite may be favoured over montmorillonite as the stable form. It is also questionable if the beidellite observed in acidic soils originates from mica and vermiculite and/or from inherent montmorillonite. Unfortunately, most investigators seem to argue the merits of one mechanism or process while ignoring most others. Most data may be interpreted with respect to more than one process. The results are therefore inconclusive as to the fate of smectites in acidic environments or if the phases are stable or metastable. Therefore, the primary thrust of the current research was to investigate the possible effects of extreme acidification, whether caused by land use practices, natural phenomena, or industrial usage, on the persistence and stability of aluminosilicate clay minerals in soils of western Canada, with particular emphasis on soil smectites.

The current investigation was initiated in pursuit of two main objectives. The first examined the hypothesis that beidellite may be produced from the incongruent dissolution of montmorillonite in acidic soil environments. Therefore the first objective was to determine if the proportion of tetrahedral substitution in smectite clay minerals is altered during weathering under acidic conditions. The second hypothesis dealt specifically with the overall stability of smectite clay in extremely acidic soil environments. Changes that occur in the chemistry of soil pore water as it percolates through a profile will influence and be influenced by the soil minerals. Dissolution, precipitation and exchange reactions all contribute to changes in the solution chemistry. Therefore the second objective was to determine if smectites found in soils of the western Canadian great plains are stable or unstable with respect to the pore water chemistry within a soil profile affected by extreme acidification.

The general approach for the study was to obtain and analyze soil samples from a field site where the native soil minerals were effected by extreme acidity, but at the same time relatively

unaffected materials of the same initial mineralogical compositions could be found in close proximity. The following five chapters that collectively make up the body of this thesis describe a sequence of experiments conducted using on a collection of soil samples obtained from a field site that met this fundamental criterion. The initial chapter in the sequence (Chapter 2) describes the chemical, mineralogical, and morphological characteristics of the soil materials at the field site. Chapter three describes the effect of acidity on the translocation of trace elements within the materials. The middle chapter in the sequence (Chapter 4) describes the changes in the chemistry of the soil solutions extracted from soil samples incubated in the laboratory at 25°C. The final two chapters (Chapters 5 and 6) describe the chemical composition, layer charge density, and calculated free energy of formation, of smectites identified in the samples and predictions for the thermodynamic stabilities of the clays with respect to equilibrated soil solutions. The collective results were used to provide insight into the stability and weathering processes of smectite in extremely acidic soil environments.

1.1 References

- Abder-Ruhman, M. 1980. Mineralogical characteristics of soils from east central Alberta. Unpublished M.Sc. thesis, University of Alberta, Edmonton, Alberta
- Badraoui, M., P.R. Bloom, and R.H. Rust. 1987. Occurrence of high-charge beidellite in a Vertic Haplaquoll of northwestern Minnesota. *Soil Sci. Soc. Am. J.* 51:813-818.
- Barshad, I. 1960a. Significance of the presence of exchangeable magnesium ions in acidified clays. *Science* 131:928-929.
- Barshad, I. 1960b. The effect of the total chemical composition and crystal structure of soil minerals on the nature of exchangeable cation in acidified clays and in naturally occurring acid soils. *Transactions of the 7th International Soil Sci. Congress, Madison WI* 2:435-444.
- Barshad, I. and A.E. Foscolos. 1970. Factors affecting the rate of the interchange reaction of adsorbed H^+ ion on the 2:1 clay minerals. *Soil Sci.* 110:52-61.
- Berg, W.A. 1986. Effects of 20 years of low N rate pasture fertilization on soil acidity. *J. Range Management* 39:122-124.
- Brunelle, A., S. Pawluk, T.W. Peters. 1976. Evaluation of profile development of some Solonchic soils of south central Alberta. *Can. J. Soil Sci.* 56:149-158.
- Bulmer, C.E. 1987. Nutrient imbalances of aspen poplar in acid sulfate soils in northwestern Alberta. Unpublished M.Sc. thesis. University of Alberta, Edmonton, Alberta.

- Carrol, D. and H.D. Starkey. 1971. Reactivity of clay minerals with acids and alkalis. *Clays and Clay Mins.* 19:321-333.
- Carson, C.D., J.A. Kittrick, J.B. Dixon, and T.R. McKee. 1976. Stability of soil smectite from a Houston black clay. *Clays and Clay Mins.* 24:151-155.
- Churchman, G.J. and M.L. Jackson. 1976. Reaction of montmorillonite with acid aqueous solutions: Solute activity control by a secondary phase. *Geochim. Cosmochim. Acta* 40:1251-1259.
- Clark, J.S. and A.J. Green 1964. Some characteristics of grey soils of low base saturation from northeastern British Columbia. *Can. J. Soil Sci.* 44:319-328.
- Cogbill, C.V. and G.E. Likens. 1974. Acid precipitation in the northeastern United States. *Water Resources. Res.* 10:1133-1137.
- Coleman, N.T. and D. Craig. 1961. The spontaneous alteration of hydrogen clay. *Soil Sci.* 91:14-19.
- Curtin, D. and A.R. Mermut. 1985. Nature and behavior of montmorillonite in an acid inland marine shale from east central Saskatchewan. *Soil Sci. Soc. Am. J.* 49:250-255.
- Douglas, L.A. 1982. Smectites in acidic soils. Page 635-640. IN H. Van Olphen and F. Veniale (eds.) *International Clay Conf. 1981. Developments in Sedimentology #35.* Elsevier, Amsterdam.
- Dudas, M.J. and S. Pawluk. 1982. Reevaluation of the occurrence of interstratified clays and other phyllosilicates in southern Alberta soils. *Can. J. Soil Sci.* 62:61-69.
- Frenkel, H., C. Amrhein and J.J. Jurinak. 1983. The effect of exchangeable cations on soil mineral weathering. *Soil Sci. Soc. Am. J.* 47:649-653.
- Grim, R.E. 1968. *Clay Mineralogy.* pg 434-444. McGraw-Hill Inc. New York.
- Hofstra, G. 1986. Acid Rain: The effects on agricultural production. *Agrologist* 15(3):6-7.
- Karathanasis, A.D. and B.F. Hajek. 1983. Transformation of smectite to kaolinite in naturally acid soil systems: Structural and thermodynamic considerations. *Soil Sci. Soc. Am. J.* 47:158-163.
- Karathanasis, A.D. and B.F. Hajek. 1984. Evaluation of aluminum-smectite stability in naturally acid soils. *Soil Sci. Soc. Am. J.* 48:413-417.
- Kittrick, J.A. 1969. Soil minerals in the Al_2O_3 - SiO_2 - H_2O system and a theory of their formation. *Clays and Clay Mins.* 17:157-167.
- Kittrick, J.A. 1971. Montmorillonite equilibria and the weathering environment. *Soil Sci. Soc. Am. Proc.* 35:815-820.
- Kittrick, J.A. 1979. Ion exchange and mineral stability: Are the reactions linked or separate. Pg. 401-412. IN E.A. Jenne (ed.) *Chemical modelling in aqueous systems: speciation, sorption, solubility and kinetics.* Am. Chem. Soc. Symp. Series. #93. Washington, D.C.

- Kodama, H. 1979. Clay minerals in Canadian soils: Origin, distribution and alteration. *Can. J. Soil Sci.* 59:37-58.
- Lietzke, D.A. and D.V. Peterson. 1987. Effects of soil acidification on chemical and mineralogical properties of a limed soil. *Soil Sci. Soc. Am. J.* 51:620-625.
- Machajdik, D. and B. Cicel. 1981. Potassium and ammonium-treated montmorillonites: II Calculation of characteristic layer charges. *Clays and Clay Mins.* 29:47-52.
- Mahler, R.L., A.R. Halvorson, and F.E. Koehler. 1985. Long-term acidification of farmland in northern Idaho and eastern Washington. *Communications. Soil Sci. Plant Anal.* 16:83-95.
- Mathers, E.P., S.W. Weed, and N.T. Coleman. 1955. The effect of acid and heat treatment on montmorillonoids. *Clays and Clay Mins.* 38:39-51.
- Mattigod, S.V. and G. Sposito. 1978. Improved method for estimating the free energies of formation of smectites. *Geochim. Cosmochim. Acta.* 42:1753-1762.
- Merino, E. and B. Ransom. 1982. Free energies of formation of illite: Solid solutions and their compositional dependence. *Clays and Clay Mins.* 38:39-51.
- Nor, Y.M. and M.A. Tabatabai. 1977. Oxidation of elemental sulfur in soils. *Soil Sci. Soc. Am. J.* 41:736-741.
- Nordstrom, D.K. 1982. Aqueous pyrite oxidation and consequent formation of secondary minerals. Pg. 37-56. IN J.A. Kittrick. et al. (eds.) *Acid sulfate weathering. Soil Sci. Soc. Am. Spec. Pub #10* Madison, WI
- Novak, I. And B. Cicel. 1978. Dissolution of smectites in hydrochloric acid: II Dissolution rate as a function of crystallochemical composition. *Clays and Clay Mins.* 26:341-344.
- Nyborg, M. 1978. Sulfur pollution in soils. Pg. 359-390. IN J.O. Nriagu, (ed.) *Sulfur in the environment: II Ecological impacts.* John Wiley and Sons. New York.
- Osthaus, B.B. 1954. Chemical determination of tetrahedral ions in nontronite and montmorillonite. *Clays and Clay Mins.* 2:341-344.
- Osthaus, B.B. 1956. Kinetic studies on montmorillonite and nontronite by the acid-dissolution technique. *Clays and Clay Mins.* 4:301-321.
- Pawluk, S. 1961. Mineralogical composition of some grey wooded soils developed from glacial till. *Can. J. Soil Sci.* 41:228-240.
- Pawluk, S. 1971. Characteristics of ferra eluviated Gleysols developed from acid shales in northwestern Alberta. *Can. J. Soil Sci.* 51:113-124.
- Pawluk, S. and M.J. Dudas. 1978. Reorganization of soil materials in the genesis of an acid Luvisolic soil of the Peace River region, Alberta. *Can. J. Soil Sci.* 58:209-220.
- Robert, M. 1973. The experimental transformation of mica toward smectite: Relative importance of total charge and tetrahedral substitution. *Clays and Clay Mins.* 23:78-80.
- Ross, G.J. and M.M. Mortland. 1966. A soil beidellite. *Soil Sci. Soc. Am. Proc.* 30:337-343.

- Senkayi, A.L., J.B. Dixon, L.R. Hossner, and L.A. Kippenberger. 1985. Layer charge evaluation of expandable soil clays by an alkylammonium method. *Soil Sci. Soc. Am. J.* 49:1054-1080.
- Sridhar, K. and M.L. Jackson. 1974. Layer charge decrease by tetrahedral cation removal and silicon incorporation during natural weathering of phlogopite to saponite. *Soil Sci. Soc. Am. Proc.* 38:847-851.
- St. Arnaud, R.J. and M.M. Mortland 1963. Characteristics of the clay fractions in a Chernozemic to Podzolic sequence of soil profiles in Saskatchewan. *Can. J. Soil Sci.* 43:336-349.
- Talibudeen, O. and K.W.T. Goulding. 1983. Charge heterogeneity in smectite. *Clays and Clay Mins.* 31:37-42.
- Weaver, R.M., M.L. Jackson. and J.K. Syers. 1971. Magnesium and silicon activities in matrix solutions of montmorillonite-containing soils in relation to clay mineral stability. *Soil Sci. Soc. Am. Proc.* 35:823-830.
- Weaver, R.M., M.L. Jackson. and J.K. Syers. 1976. Clay mineral stability as related to activities of aluminum, silicon and magnesium in matrix solution of montmorillonite-containing soils. *Clays and Clay Mins.* 24:246-252.

2. ACIDIFICATION ADJACENT TO AN ELEMENTAL SULFUR STOCKPILE: I MINERAL WEATHERING¹

2.1 INTRODUCTION

Extraction of H₂S from sour natural gas results in the production of large quantities of elemental sulfur (S°) as a by-product. More than 95% of S° produced in Canada originates in the province of Alberta from sour gas extraction (ACSCEQ 1977). Storage of recovered S° has traditionally been in the form of large stockpiles (sulfur blocks) constructed directly on the ground. Stockpiles of S° may exist for several decades before being used or sold. During the storage period some S° inevitably escapes in the form of fine wind blown particles or larger fragments that become dislodged from the sides of the block. The amount of S° deposited on soil in the vicinity of a stockpile is generally greatest immediately beside the block, decreasing with distance away from the site.

Elemental sulfur rapidly oxidizes to H₂SO₄ when applied to soil (McLean 1918; Lipman et al. 1921). The reaction is mediated under aerobic conditions by soil microorganisms, most commonly species of *Thiobacillus* (Roy and Trudinger 1970). Decreases in soil pH values depend on the amount of S° deposited on a local area, prior history of S° deposition, soil aeration, moisture content, and buffering capacity. The pH values of some Alberta soils have been shown to decline by as much as three pH units with S° application rates of up to 6.7 tonne·ha⁻¹ (Younge 1931). Soil pH values of about 2.0 have been obtained for other soils with application rates equivalent to 22 tonne·ha⁻¹ (Adamczyk-Winiarska et al. 1975).

Reclamation of S° block sites is commonly hampered by extreme acidity (pH ≤ 4.5) developed in the soil material immediately around and under stockpiles. Recently the economic demand for S° has increased dramatically, resulting in the disappearance of sulfur blocks from many gas plant sites. Limited information is available on the affects of extreme acidity on the fundamental chemical and mineralogical characteristics of soil material immediately adjacent to elemental sulfur stockpiles. Therefore the objective for this chapter was to examine the changes and redistribution of

¹A version of this chapter has been submitted for publication. C.J. Warren and M.J. Dudas 1991. Can. J. Soil Sci.

the major chemical and mineralogical components in soil material affected by extreme acidity resulting from the oxidation of large quantities of S^0 .

2.2 MATERIALS AND METHODS

Samples of surficial materials were collected from the site of a sour gas plant located about 3 km south of the townsite of Olds, Alberta in SE 1/4, section 18, township 32, range 1 west of the fifth meridian. The S^0 block had existed on the site since 1964 and, at the time of sampling, was about 10m high and covered about 1 ha. The dominant soil in the area was an Orthic Black Chernozem developed on calcareous till of continental origin. The soil solum had been stripped from the site and the block constructed on calcareous till material.

Four replicate sampling pits spaced five meters apart were excavated along the west side of the block starting 10m from the NW corner. The west side of the block was selected because the area had been continuously exposed and influenced by the block and showed no evidence of physical disturbance after the initial construction. Samples were collected in each pit from a cross sectional exposure orientated parallel to the vertical face of the block two meters from the side. Samples were collected at five cm depth increments to depths of 75 cm. Carbonates were plentiful at depths below 55 cm as identified by effervescence when treated with 10% HCl. Subsamples from selected horizons were collected separately in air tight containers to determine the gravimetric moisture content at the time of sampling. In addition, four replicate samples of the non-acidified till were collected at five meter spacings along a transect which followed a recently exposed embankment located about 50 m west of the block. These samples (identified here as the parent till) were considered representative of the calcareous till material prior to modification by the acidity derived from the sulfur block. All samples were air dried and passed through a 2 mm sieve. The samples were described according to the Canada Soil Information System (Day 1983).

Analytical values obtained for the bulk soil samples included pH in (2:1) 0.01 mol·dm⁻³ CaCl₂ (McKeague 1978), gravimetric moisture content at matrix potential of 33.3 kPa (McKeague 1978). Separate subsamples of selected layers were extracted using acid ammonium oxalate (McKeague and

Day 1966), citrate-bicarbonate-dithionite (CBD) (Mehra and Jackson 1960), and Na-pyrophosphate (McKeague 1967) extractants. The concentrations of Al and Fe in all extracts and Si in the Na-pyrophosphate extracts were determined by flame atomic absorption spectrophotometry (AAS). The content of Si in the oxalate and CBD extracts were determined colorimetrically using a heteropoly blue method (APHA 1980). Triplicate subsamples of the bulk material from selected horizons were submitted to Nuclear Activation Services Ltd. (McMaster University, Hamilton, Ontario, Canada) for the determination of total concentrations of Al, Fe, Ca, Mg, Na, K, and Ti by instrumental neutron activation analysis (INAA). The content of Si in each sample was calculated by difference. The content of total inorganic carbon (carbonate) in the bulk samples was determined using the procedure of Bundy and Bremner (1972). X-ray diffractograms for selected specimens were obtained as random powder mounts.

Subsamples from all sampled horizons were dispersed in distilled water using ultrasonic vibration (Genrich and Bremner 1972) and separated into sand (2.0 - 0.05 mm), silt (0.05 - 0.002 mm), and clay (<0.002 mm) size fractions by repeated gravity sedimentation and wet sieving (Jackson 1979). The quantities of sand and silt were determined from the mass of the oven dry separates. Clay content was calculated by difference.

To quantify the amounts of feldspars in the sand fraction, subsamples of the oven dried sand separates were further separated into heavy (densities greater than $2.76 \text{ Mg}\cdot\text{m}^{-3}$) and light (densities less than $2.76 \text{ Mg}\cdot\text{m}^{-3}$) fractions by a sink-float method using a mixture of tetrabromoethane and nitrobenzene (Jackson 1979). Samples of the light mineral fraction were dissolved (Appendix A) and the digests analyzed for content of Ca, Na, and K by AAS. The resultant data were used to calculate the percentages of Ca, Na, and K feldspars with the remaining percentage in the light mineral fraction allocated to quartz.

Phyllosilicate minerals present in the clay separates were identified from X-ray diffractograms of orientated specimens. Subsamples of the separated clay-size fraction were saturated with Ca^{2+} and K^{+} by repeated treatments with $1 \text{ mol}\cdot\text{dm}^{-3}$ solutions of the respective chloride salts. Samples were washed free of excess electrolyte by repeated dispersion in distilled water and centrifugation. Oriented

specimens of the electrolyte free Ca^{2+} - and K^{+} -saturated clay separates were prepared using the paste method (Thiesen and Harward 1962) and subjected to seven pretreatments as described by Dudas and Pawluk (1982). Diffraction patterns were obtained on a Philips step-scanning diffractometer using a step size of $0.05^\circ 2\theta$ and an accumulation time of 2 seconds $\cdot\text{step}^{-1}$. All samples were irradiated with $\text{Co K}\alpha$ radiation ($\lambda = 0.17903 \text{ nm}$) generated at 50 kV and 25 mA.

The dominant 2:1 phyllosilicates identified in the clay separates were quantified using a combination of physical and chemical determinations. The surface area of the clay separates was determined by adsorption of ethylene glycol monoethyl ether (EGME) using the method of Carter et al. (1965) and incorporating the modifications of Dudas and Pawluk (1982). The total cation exchange capacity was determined by extracting subsamples of the electrolyte free Ca^{2+} -saturated clays with neutral $1 \text{ mol}\cdot\text{dm}^{-3} \text{ NaCl}$ and determining the concentration of Ca in the extracts by AAS (McKeague 1978). To determine the potassium fixing ability of the minerals in the clay separates and provide an estimate of vermiculite content, subsamples of the electrolyte free K^{+} -saturated clays were dried at 105°C and resaturated with Ca by repeated washings with $1 \text{ mol}\cdot\text{dm}^{-3} \text{ CaCl}_2$ followed by repeated dispersion in distilled water and centrifugation to remove excess electrolyte. Samples of both Ca^{2+} -saturated specimens and Ca^{2+} -resaturated, K^{+} -saturated specimens were dissolved in HF and HNO_3 (Appendix A). Digests were analyzed for content of K by AAS.

The quantities of kaolinite and chlorite in the clay separates were estimated using X-ray diffraction data. The quantity of kaolinite in each clay separate was estimated by determining the area under the (001) reflections (0.715 nm peak). Areas were estimated numerically using a midpoint Riemann sum (Fraleigh 1985) by taking subintervals equal in width to the $0.05^\circ 2\theta$ step size and equal in height to the difference between measured counts $\cdot\text{second}^{-1}$ for each step and the mean counts $\cdot\text{second}^{-1}$ for the background. The areas under the reflections were determined for 25 steps on either side of the maximum. Mean background values were calculated from five steps on either side of the maxima outside of the above mentioned range. The quantities of kaolinite in each sample were estimated by comparing areas obtained from the diffractograms of the Ca^{2+} -saturated specimens with data obtained from diffractograms of Ca^{2+} -saturated samples prepared from a series of artificial mixtures containing

known masses of a standard Georgia kaolinite and Chambers montmorillonite (API standards #3 and #23, respectively; Kerr et al. 1950). The quantity of kaolinite in the artificial mixtures ranged from 50 g·kg⁻¹ to 300 g·kg⁻¹. It was assumed that the kaolinite identified in the samples was of uniform crystallinity (Chittleborough and Walker 1988) and contributions to the area under the peak from second order reflections of chlorite were not significant. Criteria for the presence or absence of chlorite in the clay separates was based on the presence, absence, and intensity of the 1.4 nm peak in the diffractograms for the K⁺-saturated, 105°C and 550°C pretreated specimens.

2.3 RESULTS AND DISCUSSION

2.3.1 Profile Characteristics

The number, arrangement, thickness, and field appearance of layers within the profiles exposed in all four pits were very similar. A description representative of soil samples obtained from 5 cm depth increments is given in Table 2.1. Three distinct soil layers were identified within the profile. The surface material to 45 cm depth was uniformly grey (10YR 6/1 d) and extremely acidic with pH values ranging between 1.6 and 3.0. Below the acidic surface material was a 15 cm thick, reddish colored, Fe-enriched, indurated layer overlying calcareous material containing up to 120 g·kg⁻¹ CaCO₃ equivalent.

The pH values (2:1 0.01 mol·dm⁻³ CaCl₂) of the surface layer ranged between 1.6 and 2.9 with a modal value of 2.1. The pH range included the theoretical value for the second dissociation constant for H₂SO₄ (Lindsay 1979):



indicating that HSO₄⁻ was a dominant species in the soil solution. The total amount of dissolved sulfate was therefore at least partially responsible for buffering the soil pH around 2.1.

Table 2.1 Description and some chemical properties of soil samples at 5 cm depth increments representative of the profile exposed at a distance of two meters from the edge of the sulfur block.

Depth (cm)	Color (dry)	Text.	Structure	Consistence (moist, dry)	pH	Carbonate [*] (CaCl ₂) (g·kg ⁻¹)
0-5	Gray (10YR 6/1)	CL	amorphous	v. friable, soft	1.6	0.0
5-10	Gray (10YR 6/1)	CL	amorphous	v. friable, soft	2.0	0.0
10-15	Gray (10YR 6/1)	CL	amorphous	v. friable, soft	2.1	0.0
15-20	Gray (10YR 6/1)	CL	amorphous	v. friable, soft	2.2	0.0
20-25	Gray (10YR 6/1)	CL	amorphous	v. friable, soft	2.2	0.0
25-30	Gray (10YR 6/1)	CL	amorphous	v. friable, soft	2.1	0.0
30-35	Gray (10YR 5/1)	CL	amorphous	v. friable, soft	2.1	0.0
35-40	L. Brownish Gray (2.5Y 6/2)	CL	amorphous	v. friable, soft	2.3	0.0
40-45	L. Yellowish Brown (2.5Y 6/4) **	CL	amorphous	v. friable, soft	2.9	7.0
45-50	Red (2.5YR 5/6)	L	coarse platy	ext. hard, indurated	3.8	3.2
50-55	Reddish Yellow (5YR 6/6)	L	coarse platy	ext. hard, indurated	5.5	16
55-60	L. Yellowish Brown (2.5Y 6/4)	L	amorphous	firm, hard	6.6	56
60-65	L. Olive Brown (2.5Y 5/4)	CL	amorphous	firm, hard	6.8	72
60-70	Pale Yellow (2.5Y 7/4)	CL	amorphous	firm, hard	7.3	100
70-75	Pale Yellow (2.5Y 7/4)	CL	amorphous	firm, hard	7.6	103
Parent	L. Gray (10YR 7/2)	L	amorphous	firm, hard	7.8	187
Till						

* Expressed as CaCO₃ equivalent.

** Sample from one pit contained a few fine faint pale yellow (2.5Y 7/4 m) mottles.

The acidified surface material contained the chemically weathered, friable remains of some rock fragments up to 25 cm in diameter. Most were encased in white (10YR 8/1 m) coatings one to two mm thick. Discrete nodules similar in composition to the rock coatings and up to five cm in diameter were also observed within the acidified surface layer. X-ray diffraction patterns for samples of the nodules and the rock coatings displayed strong reflections at 0.756, 0.306, 0.428, 0.380, and 0.280 nm identifying the material as gypsum ($\text{CaSO}_4 \cdot 2\text{H}_2\text{O}$).

The reddish colored indurated layer directly underlying the acidic material displayed a coarse platy structure (Table 2.1). The thickness of the layer ranged from 10 to 15 cm. The boundary between the acidic surface layer and the indurated layer at about 45 cm depth was smooth and abrupt. Samples obtained from just above the indurated layer, at depths between 40 and 45 cm, displayed a yellowish (2.5Y) hue. Samples collected at the 40-45 cm depth from one of the pits also contained a few small pale yellow mottles (Table 2.1). X-ray diffractograms obtained for samples of the mottles displayed weak reflections at 0.594, 0.574, 0.509, 0.308, and 0.229 nm indicating the presence of jarosite ($\text{KFe}_3(\text{SO}_4)_2(\text{OH})_6$). X-ray diffraction was also used to identify gypsum, hematite, and calcite in the indurated layer.

Carbonate contents increased from the top of the indurated layer with increasing depth as hues decreased in redness (Table 2.1). The calcareous layer underlying the reddish colored indurated layer at depths greater than 65 cm contained up to $120 \text{ g} \cdot \text{kg}^{-1} \text{ CaCO}_3$ equivalent with pH values ranging between 7.0 and 8.0. Samples of the parent till obtained at 50 m away from the sulfur block displayed pH values of 7.8 and equivalent CaCO_3 contents between 170 and $200 \text{ g} \cdot \text{kg}^{-1}$.

Although the characteristics of the three layers of weathered soil material were similar for all four exposed profiles, the thickness of the acidic surface layer and the depth to the top of the indurated reddish colored layer decreased with increasing distance from the side of the block. The orientation and thickness of materials with respect to the edge of the sulfur block are illustrated in Figure 2.1. The reddish colored indurated layer was observed at the soil surface at distances of about three meters from the wall of the block. At distances further than three meters vegetation was common and carbonates were observed at the surface. At distances closer than three meters to the side of the block the soil

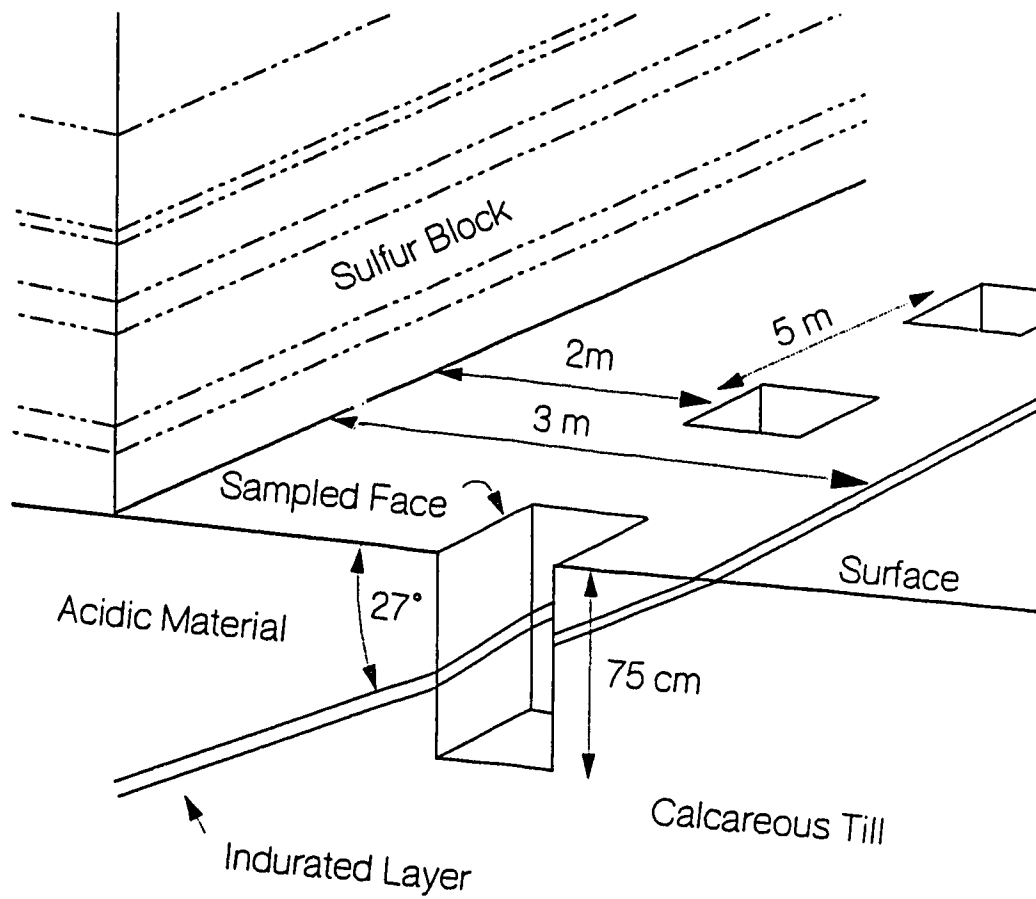


Figure 2.1 Schematic three dimensional diagram of the sample site indicating the position and orientation of the sample pits with respect to the elemental sulfur block and a cut away section displaying the orientation of the sampled materials and layers. Not to scale.

surface was devoid of vegetation and littered with chunks of S° ranging in diameter from less than 2 mm to greater than 50 cm. The thickness of the acidified soil layer and the depth at which the indurated layer was encountered increased by about 50 cm for every meter of approach to the face of the block. The slope of the incline (angle of dip) was estimated at about 27 degrees towards and under the block (Figure 2.1).

The inward slope of the indurated layer was likely the result of concentrated runoff of meteoric waters from the stockpile and oxidation of large quantities of S° dislodged from the sides. The increased throughflow of water along the sides of the block promoted the deeper advancement of the acid front. Once developed, the indurated layer impeded downward flow of water into the underlying calcareous material. At the time of sampling, the acidified layer contained an average gravimetric moisture content of $0.36 \text{ g}\cdot\text{g}^{-1}$ while the calcareous layer contained only $0.18 \text{ g}\cdot\text{g}^{-1}$. This compared with gravimetric moisture contents of 0.29 and $0.25 \text{ g}\cdot\text{g}^{-1}$ at tensions of 33.3 kPa (field capacity) determined using the pressure plate apparatus for disturbed samples of the acidified and calcareous materials, respectively. Samples obtained with a hand auger to depths of up to two meters at random locations around the stockpile and at various distances from the edge of the block indicated that the slope and orientation of the indurated layer were consistent around the perimeter of the stockpile. As a result of this inward sloping feature, the areal extent of material influenced by the process of extreme acidification was confined to the surface soil layer within a few meters of the sides of the block and directly underneath. The total volume of acidified soil material surrounding the entire block was estimated at about 950 m^3 .

Differences in the total concentrations of major constituents with depth indicated selective dissolution and downward translocation of some elements (Table 2.2). The concentration of Fe and Mg in the acidified material was reduced to between 10% and 30% of the content of the parent till. Iron dissolved from the acidified material was deposited in the indurated layer between 45 and 55 cm depth. Precipitation of Fe occurred in response to an increased pH environment due to reaction with carbonate at depth. Magnesium displayed no similar enrichment within the profile indicating that the solubility of epsomite ($\text{MgSO}_4\cdot 7\text{H}_2\text{O}$) or any other Mg sulfate solid was not exceeded. The

concentration of Ca in the zero to five cm depth layer was reduced by about 25% compared to the underlying calcareous material and enriched by a similar percentage at depths between 40 and 50 cm (Table 2.2) indicating some accumulation of Ca in the lower part of the acidified layer at the interface with the indurated layer. Silicon (SiO_2) and Na_2O were enriched in the upper portion of the acidified layer compared to the parent till due to selective removal of other elements, primarily Fe and Mg. The total content of Al_2O_3 , K_2O , and TiO_2 in the sampled materials displayed significant differences ($P = 0.05$) among depths but trends within the profile were not evident.

Table 2.2 Chemical composition of bulk soil samples from selected depths in the profile at a distance of two meters from the edge of the block. Values within each column followed by the same letter are not significantly difference ($P = 0.95$, Tukey's HSD interval, $n = 3$).

Depth (cm)	SiO_2	Al_2O_3	Fe_2O_3	MgO ($\text{g}\cdot\text{kg}^{-1}$)	K_2O	TiO_2	CaO	Na_2O
0-5	830 cd	84 b	6.5 a	3.5 a	15 bcd	5.0 b	46 a	6.3 c
20-25	840 d	47 a	7.7 a	4.5 a	15 cde	4.2 ab	65 ab	6.6 c
40-45	800 bc	80 ab	14 a	4.5 a	13 ab	4.4 ab	75 b	6.0 bc
45-50	760 a	63 ab	47 d	26 c	12 a	3.3 a	80 b	5.2 abc
60-65	770 ab	84 b	34 c	21 b	16 de	4.2 ab	58 ab	4.3 a
70-75	780 ab	75 ab	29 bc	25 cd	17 e	4.6 b	61 ab	4.6 ab
Parent Till	780 ab	70 ab	23 b	28 d	13 abc	4.1 ab	76 b	4.7 ab

The quantities of pyrophosphate, oxalate, and citrate-bicarbonate-dithionite (CBD) extractable Fe (Fe_p , Fe_o , and Fe_d , respectively) in the profile reflected the content of total Fe (cf. Tables 2.2 and 2.3). The quantities of extractable Al displayed a similar trend to Fe but did not follow the total content of Al in the samples. Extractable levels of both Fe and Al were generally lower in the acidic

layer and enriched in the indurated layer relative to the calcareous material. The content of Fe_o was similar to the content of Fe_p in the upper 25 cm of the acidified surface but lower than the content of Fe_d . The amount of pyrophosphate extractable Al (Al_p) in the acidic samples exceeded the content of both CBD extractable Al (Al_d) and oxalate extractable Al (Al_o) by about one order of magnitude. This suggested that much of the extractable Al in the acidified material may have been bound to organic material or combined with amorphous Si, while extractable Fe was primarily associated with mineral material.

Table 2.3 Mean ($n = 3$) concentrations ($g \cdot kg^{-1}$) of Fe, Al, and Si extracted from selected samples by Na pyrophosphate (Pyro), acid ammonium oxalate (Ox) and citrate-bicarbonate-dithionite (CBD) methods.

Depth ----- (cm)	Fe			Al			Si		
	Pyro	Ox	CBD	Pyro	Ox	CBD	Pyro	Ox	CBD
0-5	0.53	0.58	0.67	5.0	0.57	0.57	23	0.02	5.1
20-25	0.67	0.62	1.7	6.6	0.87	0.61	28	0.03	4.7
40-45	1.2	4.1	5.4	6.6	0.84	0.72	25	0.03	4.8
45-50	3.5	28	23	11	14	12	5.0	2.0	1.4
60-65	1.8	11	9.4	7.1	4.8	4.5	9.3	1.8	1.2
70-75	2.5	8.1	7.0	7.2	2.5	1.3	16	1.8	1.1
Parent Till	1.2	6.9	4.8	4.6	1.6	0.65	12	1.4	0.93

Quantities of Fe_o and Al_o in the indurated layer (45-50 cm depth) equalled or exceeded the Fe_d and Al_d contents at depths below 50 cm. The content of Fe_o also greatly exceeded the content of Fe_p , however, the content of Al_p was greater than or equal to the content of Al_o . The high amount of Fe_o in the indurated layer compared to other extractable forms suggested that much of the Fe precipitated in the indurated layer occurred as amorphous oxides and/or hydroxides. The presence of some hematite in

the indurated layer, as identified by X-ray diffraction, was likely due to the transformation of rapidly precipitated amorphous Fe under neutral pH conditions (Schwertmann and Murad 1983; Goss 1987). The high content of Al_p in the indurated layer relative to other extractable forms suggested that Al mobilized within the acidified layer accumulated in the indurated layer in association with organic material or in association with amorphous Si. Two separate mechanisms of metal translocation, commonly associated with podzolization, were therefore possibly responsible for translocation of Fe and Al in the profile.

The color, thickness, and texture of the indurated layer met the criteria for a Podzolic B horizon (CSSC 1978). The chemical values for $Al_p + Fe_p$, total content of Fe_p , ratio of $(Al_p + Fe_p)$:clay, total content of organic carbon ($12 \pm 5 \text{ g}\cdot\text{kg}^{-1}$), and ratio of organic carbon: Fe_p further indicated that the layer met the criteria for a Podzolic Bf horizon. The indurated character of the material and the thickness of the layer suggested that it may be similar to an Podzolic ortstein horizon designated Bfc.

2.3.2 Primary Minerals

Chemical weathering of soil minerals within the profile proceeded first with the dissolution of carbonates followed by the dissolution of Fe containing primary and secondary minerals. Carbonate minerals buffered the pH values between 7.0 and 8.0 and would be completely dissolved before pH values decreased into the acid range where the solubility of Fe greatly increases and Fe-containing minerals dissolve. It was assumed that the carbonate content of the parent till within the local area was uniform (approximately $190 \text{ g}\cdot\text{kg}^{-1} \text{ CaCO}_3$ equivalent) prior to establishment of the block. The reasonably uniform content of TiO_2 in the profile (Table 2.2) with depth suggested that there were no major lithological changes in the soil column. Carbonate minerals found in the parent till and any carbonate material that may have been applied to the surface as part of remedial procedures were consumed through reaction with H_2SO_4 . Calcium dissolved from carbonate, plagioclase feldspars, and other Ca containing minerals precipitated with sulfate to form gypsum in the acidified layer. The content of carbonate in the calcareous material was also reduced compared to the content of samples of

the parent till obtained about 50 m from the stockpile (Table 2.1). This indicated that the amount of carbonate below the indurated layer was reduced through reaction with acidic solution at some time during the chemical weathering process.

Preferential acid attack of feldspars and heavy minerals in the sand fraction was evident in their reduced abundance in the acidified layer relative to the parent till (Table 2.4). The content of quartz in the sand fraction of the acidified layer displayed a concomitant increase reflected in the increase in the total amount of SiO_2 (Table 2.2). The content of heavy minerals in the acidified surface layer was reduced to about one-fifth the content in the parent till (Table 2.4) which was also reflected in the reductions in the total content of Fe and Mg in the acidified material (Table 2.2). Some of the Mg dissolved from the acidified material was also likely associated with carbonate minerals initially present. The amount of feldspars remaining in the acidified layer compared to the underlying calcareous material was greater than for the heavy mineral fraction, indicating less dissolution of the feldspars under conditions of extreme acidity. Calcium feldspars in the acidified layer were preferentially dissolved compared to the Na- and K-feldspars. The content of Ca-feldspar in the 0 to 10 cm layer was about one-third the content of the underlying calcareous till material while the contents of Na- and K-feldspars at the same depth were about two-thirds the levels in the calcareous till.

Constituents dissolved under conditions of extreme acidity were deposited within the profile as a variety of secondary minerals. Calcium derived largely from the dissolution of carbonates and plagioclase feldspars reacted with sulfate to form gypsum. Some downward movement of Ca was evident by the slight reduction in the content of Ca in the 0 to 5 cm layer and slight enrichment of Ca in the lower layers of the acidified material just above the indurated layer (Table 2.2). Evidence of minimal leaching of Ca and the gypsum crusts observed around most rock fragments in the acidified layer indicated that precipitation of gypsum was rapid. Slow precipitation of gypsum would also likely produce large crystals of selenite similar to those found in acid sulfate soils (Pawluk 1971). Selenite crystals were not observed in any of the samples from the present study. The presence of jarosite in the profile suggested dissolution of some K containing minerals. However, this was not evident from the total content of K in the samples (Table 2.2). The primary source of K used to form jarosite was likely

exchangeable K and the dissolution of K feldspars. Formation of jarosite within some profiles just above the indurated layer indicated that downward leaching and accumulation of K was required for jarosite to form.

Table 2.4 Mean mineralogical composition of the sand fraction from selected depths in the profile.

Values within a mineral group followed by the same letter are not significantly different (P = 0.95, Tukey's HSD interval, n=4).

Depth (cm)	Feldspars			Quartz	Heavy Minerals
	K	Na	Ca (g·kg ⁻¹)		
0-5	55 a	74 a	17 a	850 e	6.9 a
5-10	62 ab	87 abc	19 a	820 e	6.3 a
20-25	66 ab	98 abc	27 ab	800 de	8.3 a
35-40	60 ab	84 ab	34 bc	810 de	8.5 a
40-45	71 bc	99 abc	46 cd	750 cd	27 ab
45-50	83 cd	120 c	56 d	700 bc	40 b
50-55	87 d	120 c	52 d	650 b	79 c
60-65	88 de	110 bc	47 cd	700 bc	38 b
70-75	90 de	150 d	60 d	650 b	30 ab
Parent Till	100 e	160 d	99 e	580 a	40 b

Extractable levels of Al and Si in the samples from the 40-45 cm depth suggested the presence of amorphous secondary aluminosilicates within the profile (Table 2.3). Based on the calculation procedures for pyrophosphate and oxalate extractable levels of Al and Si outlined by Parfitt and Kimble (1989) the Al/Si ratio for the 45 to 50 cm depth sample was 1.1 suggesting the possible presence of allophane in the sample. However, the pH value for the sample was lower than 4.7 (Table 2.1)

indicating the allophane would not likely precipitate in the acidic material. The surface area and cation exchange capacity for the clay separates from the same depth (Table 2.5) did not indicate the presence of this secondary mineral.

2.3.3 Clay Minerals

Physical, chemical, and X-ray diffraction data collected for the clay separates indicated that the calcareous till material initially contained a suite of clay minerals common to soils of the Interior Plains (Kodama 1979; Dudas and Pawluk 1982). The extreme acidity developed in the surface layer resulted in dissolution and alteration of some of the phyllosilicates.

X-ray diffractograms obtained for all specimens of the clay separates displayed strong sharp reflections with peaks at 0.715 and 0.997 nm indicative of the presence of kaolinite and discrete unaltered mica (Figure 2.2). The content of K in the clay separates did not change significantly ($P > 0.05$) with depth (Table 2.5) indicating that clay-sized mica was not affected by the extreme acidity. X-ray diffraction patterns for the Ca^{2+} -saturated clay separates also displayed second order (002) peaks for mica at 0.498 nm indicative of the dioctahedral (muscovite) variety of mica (Fanning and Keramidas 1977).

Data for potassium content for the Ca^{2+} -saturated and Ca^{2+} -resaturated K^{+} -saturated clay separates (Table 2.5) provided estimates for the content of mica and vermiculite in the clay fraction. Values obtained for the potassium content of the clay separates ranged between 20 and 30 $\text{g}\cdot\text{kg}^{-1}$ for both the Ca^{2+} -saturated and Ca^{2+} -resaturated K^{+} -saturated samples. In the case of the Ca^{2+} -saturated separates the values corresponded to a range in the mica content of between 250 and 340 $\text{g}\cdot\text{kg}^{-1}$ (mean = $315 \pm 28 \text{ g}\cdot\text{kg}^{-1}$), assuming 100 $\text{g}\cdot\text{kg}^{-1}$ K_2O in pure mica (Mehra and Jackson 1959). Differences in the content of potassium of the clays were not significant ($P > 0.05$) between the Ca^{2+} -saturated and Ca^{2+} -resaturated K^{+} -saturated treatments or among values within each treatment indicating no changes in either the total content of mica in the profile or formation of vermiculite due to alteration of 2:1 phyllosilicates.

Table 2.5 Some physical and chemical characteristics, quantitative estimates of kaolinite, and semi-qualitative estimates of chlorite in the total clay separates from selected depths.

Values within a column followed by similar letters are not significantly different

($P = 0.95$, Tukey's HSD interval, $n=4$).

Depth (cm)	Surface Area ($\text{m}^2 \cdot \text{g}^{-1}$)	Cation Exch. Capacity ($\text{cmol}(+) \cdot \text{kg}^{-1}$)	K Content *		Kaolinite ($\text{g} \cdot \text{kg}^{-1}$)	Chlorite **
			Ca-Sat ———— (g·kg ⁻¹)	K-Sat ————		
0-5	454 a	30 def	28	27	86 abc	-
5-10	450 a	34 cde	28	28	110 ab	-
20-25	437 ab	36 bcd	27	28	110 ab	+
35-40	413 abc	41 ab	26	27	72 bc	+
40-45	403 bc	40 abc	27	28	74 abc	+
45-50	335 de	28 fg	24	25	64 c	+ + +
50-55	304 e	24 g	21	22	110 ab	+ + +
60-65	408 abc	29 efg	27	27	91 abc	+ +
70-75	428 abc	42 a	27	27	120 a	+ +
Parent Till	367 cd	39 abc	27	27	110 ab	+ +

* No significant differences ($P = 0.05$) between treatments or among values within each treatment.

** Symbols: (-) absent, (+) trace present, (+ +) equal to content in the parent till, (+ + +) greater than content in parent till.

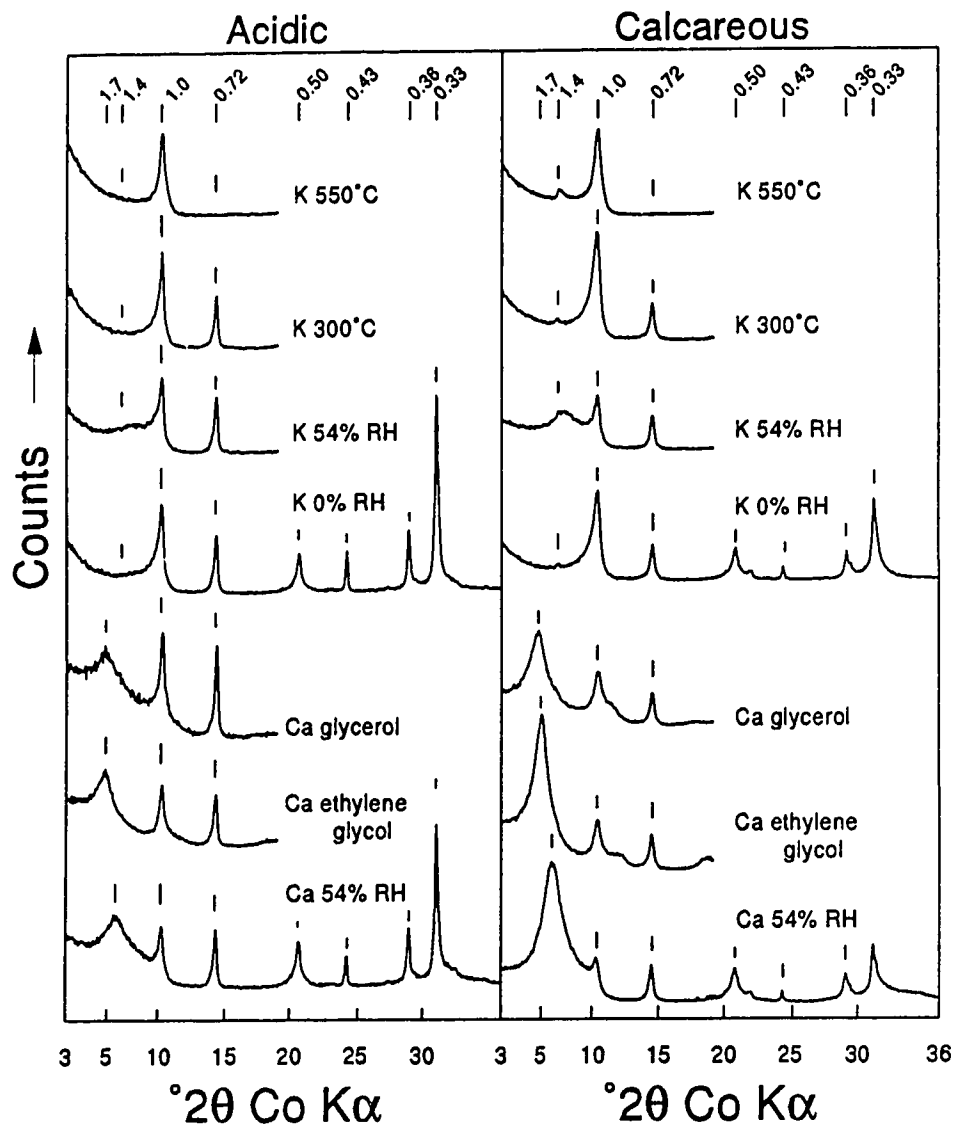


Figure 2.2 X-ray diffractograms obtained for Ca-saturated and K-saturated clay specimens from the acidified (0 to 5 cm depth) and calcareous parent till obtained 50 m from the block. Diffractograms of the Ca-saturated clay separates were obtained under conditions of 54 % relative humidity (Ca 54%RH) and after pretreatments with glycerol (Ca Gly) and ethylene glycol (Ca EG). Diffractograms of the K-saturated clay separates were obtained under conditions of 54 % RH (K 54%RH), and under conditions of 0 % RH after heating to 105°C (K 0%RH), 300°C (K 300), and 550°C (K 550). Values along the top indicate approximate d-spacing positions in nanometers.

The content of kaolinite in the clay fraction was also not altered by the extreme acidity of the surface material. The content of kaolinite in the clay fraction (Table 2.5), based on the areas under the 0.715 nm X-ray diffraction peaks, ranged from 64 to 120 g·kg⁻¹. The empirical mathematical relationship between peak area (PA) and kaolinite content (KAO) for the prepared artificial standards was:

$$\text{KAO (g·kg}^{-1}\text{)} = \text{PA} \times 0.35 + 18 \quad R^2 = 0.96 \quad [2.2]$$

The highest concentrations of kaolinite were observed in the calcareous till material which contained amounts not significantly ($P = 0.05$) different from the kaolinite content of the acidified surface layer. Samples from the indurated layer and the lower layers of the acidified material contained lower quantities of kaolinite. Reduction in the content of kaolinite in the indurated layer was attributed primarily to dilution because of the accumulation of secondary Fe minerals.

Chlorite was totally removed from the upper portions of the acidified layer. Weak reflections at 1.4 nm in the K⁺-saturated specimens corresponding to discrete chlorite were observed in samples from the calcareous parent till, but were absent in samples from the upper portion of the acidified surface layer (Figure 2.2, Table 2.5). Similar 1.4 nm peaks were barely discernible in patterns obtained for the lower portion of the acidified material (data not shown).

Removal of chlorite from the acidified material may have been due to removal of the hydroxy-interlayer and/or total dissolution. Dissolution of the hydroxy-interlayer results in the transformation of chlorite to interstratified 2:1 clays, vermiculite, smectite, or other 2:1 phyllosilicates of intermediate charge density (Ross and Kodama 1973; Senkayı et al. 1981; Dixon et al. 1982). Lack of an increase in the K fixing ability for the clays of the upper portion of the acidified layer (Table 2.5) suggested that dissolution of the hydroxyl layer resulted in the formation of smectite rather than vermiculite. Increases in the intensity of the 1.4 nm peaks on heating to 550°C (Figure 2.2) indicated that the chlorite native to the parent carbonate till was Fe-rich (Bailey 1988). Iron substitution in both the hydroxy-interlayer and the 2:1 units of the structure is required for the transformation of chlorite to smectite (Senkayı et al. 1981). Ross (1969) demonstrated that chlorites dissolve congruently in acidic

solution at rates that increase with increasing structural content of Fe and decreasing content of Mg. If dissolution of hydroxy-interlayer occurred, the resulting 2:1 structure was indistinguishable from other smectites in the acidified material because the total amount of chlorite in the samples was small. The contribution of chlorite, once weathered, to the total quantity of 2:1 phyllosilicates in the clay fraction would not be substantial. Although both mechanisms for the destruction of the chlorite may have been active in the acidified material, conclusive evidence favouring either mechanism was not evident.

Slight differences were observed between reflections for the 2:1 expanding clays separated from the acidified layer and the calcareous material suggesting selective acid attack of the smectite structure. Expandable 2:1 phyllosilicates in the Ca^{2+} -saturated specimens separated from the calcareous material displayed basal spacings of 1.70 and 1.71 nm with pretreatments of ethylene glycol and glycerol, respectively (Figure 2.2). These clays also displayed rehydration of the K^{+} -saturated specimen after oven drying for 24 h at 105°C. Such behavior was indicative of the presence of montmorillonite in the sample. The Ca^{2+} -saturated clay specimens separated from the acidified layer also displayed expansion to spacings of 1.70 and 1.71 nm with ethylene glycol and glycerol pretreatments, respectively, but the K^{+} -saturated specimens from the acidified layer displayed only limited rehydration (K 54%RH) after oven drying suggesting an increase in the charge density of the 2:1 structure and/or a shift in the tetrahedral:octahedral ratio. Intensities for the 1.7 and 1.4 nm peaks for the Ca^{2+} -saturated specimens from the acidified layer were also lower in intensity relative to the 0.72 and 1.0 nm peaks. Similar reflections for smectite for specimens from the calcareous material were higher than the reflections for the dioctahedral mica and kaolinite.

Data for surface area and cation exchange capacity provided quantitative estimates for the amount of smectite in the clay separates (Table 2.5). Values for total surface area of clay separates ranged from about 450 $\text{m}^2\cdot\text{g}^{-1}$ in the surface layer, 300 $\text{m}^2\cdot\text{g}^{-1}$ in the indurated layer, and between 370 and 430 $\text{m}^2\cdot\text{g}^{-1}$ in the parent till. These values corresponding to smectite contents of 550, 370, and between 450 and 525 $\text{m}^2\cdot\text{g}^{-1}$, respectively, assuming a surface area of 820 $\text{m}^2\cdot\text{g}^{-1}$ for pure smectite and that only smectite contributed significantly to the measured surface area. Values for the cation exchange capacity for the surface, indurated and calcareous layers were 30, 24, and 42 $\text{cmol}(+)\cdot\text{kg}^{-1}$,

respectively. The low values for surface area and cation exchange capacity for the clays from the indurated layer relative to the calcareous material was attributed to precipitation of Fe and Al in the interlayer of 2:1 phyllosilicates as indicated by the increase in the amount of chlorite in the indurated layer. The slightly higher values for surface area values for the clays from the acidic samples compared to the calcareous material suggested an increase in the smectite content of the acidified layer. The presence of large amounts of amorphous Si in the acidified material, as indicated by the large amount of pyrophosphate extractable Si (Table 2.3), may account for the observed increase in the surface area values over the calcareous material. Reduction in the first order reflections for smectite in the X-ray diffractograms for the clay specimens from the acidified layer compared to the first order reflections for mica and kaolinite (Figure 2.2) indicated that the total content and/or the degree of crystallinity of smectite in the acidified layer was reduced relative to the smectites in the calcareous material.

2.4 CONCLUSIONS

Acidification of soil material adjacent to elemental sulfur blocks results in the formation of three zones of weathering: an extremely acidic surface layer and an Fe-rich indurated layer, overlying calcareous parent material. Chemical weathering in the surface material at pH values about 2.1 resulted in the selective dissolution of carbonates, Fe-containing primary minerals, chlorite, and to a lesser extent plagioclase feldspars. Smectites were also attacked under extremely acidic conditions resulting in a decrease in the total content of smectite in the surface layer and/or the degree of crystallinity of smectite. X-ray diffraction data also suggested a slight increase in the mean tetrahedral:octahedral charge ratio of the smectite. Formation of vermiculite structures either from the depotassification of mica or the transformation of smectite was not evident. Copious quantities of finely divided gypsum formed within the acidified layer at the expense of calcium carbonate and Ca-feldspars. Iron derived from chlorite and Fe-containing primary minerals was translocated and deposited at the interface between acidic and calcareous materials primarily as amorphous oxides and hydroxides. Transformation of some precipitated Fe to hematite was also evident. Precipitation and accumulation of Fe resulted in the formation of a very hard, indurated layer about 10 to 15 cm thick. The layer was

sloped at about 27 degrees towards and under the side of the block and diverted downward flow of water under the stockpile. The layer displayed the characteristics of an ortstein (Bfc) horizon. Jarosite precipitated within the profile just above the indurated layer. Precipitation of allophane in the acidified material just above the indurated layer was not evident. The geometry of the indurated layer, with its inwards sloping orientation contributed to retardation of the spreading of acid drainage waters from the stockpile.

2.5 REFERENCES

- Adamczyk-Winiarska, Z., Krol, M., and Kobus, J. 1975. Microbial oxidation of elemental sulphur in Brown soil. *Plant and Soil* 43:95-100.
- American Public Health Association (APHA). 1980. Standard methods for the examination of water and wastewater. 15th ed. Am. Public Health Assoc., New York, p426-436.
- Associate committee on scientific criteria for environmental quality (ACSCEQ). 1977. Sulphur and its inorganic derivatives in the Canadian environment. NRCC #15015, National Research Council of Canada. Ottawa. 426 pp.
- Bailey, S.W. 1988. Chlorites: Structures and crystal chemistry. Pages 347-404. IN S.W. Bailey, (ed.) Hydrous phyllosilicates (exclusive of micas). *Reviews in mineralogy* Vol. 19, Min. Soc Am. Wash. D.C.
- Bundy, L.G. and Bremner, J.M. 1972. A simple titrimetric method for determination of inorganic carbon in soils. *Soil Sci. Soc. Am. Proc.* 36:273-275.
- Canada Soil Survey Committee, Subcommittee on Soil Classification (CSSC). 1978. The Canadian system of soil classification. Can. Dep. Agric. Publ. 1646. Supply and Services Canada, Ottawa, Ont. 164pp.
- Carter, D.L., Heilman, M.D. and Gonzalez, C.L. 1965. Ethylene glycol monoethyl ether for determining surface area of silicate minerals. *Soil Sci.* 100:356-360.
- Chittleborough, D.J. and Walker, P.H. 1988. Crystallinity of soil kaolinites in relation to clay particle-size and soil age. *J. Soil Sci.* 39:81-86.
- Day J.H. (ed.) 1983. The Canada soil information system (CanSIS): Manual for describing soils in the field, 1982 revised. Expert Committee on Soil Survey. Land Resource Research Institute, Ottawa, p 64-86.
- Dixon, J.B., Hossner, L.R., Senkayi, A.L. and Egashira, K. 1982. Mineralogical properties of lignite overburden as they relate to mine spoil reclamation. Pg. 169-191. IN J.A. Kittrick, D.S. Fanning, and L.R. Hossner, (eds.) *Acid sulfate weathering*. Soil Sci. Soc. Am. Pub. Madison, WI.
- Dudas, M.J. and Pawluk, S. 1982. Reevaluation of the occurrence of interstratified and other phyllosilicates in southern Alberta soils. *Can. J. Soil Sci.* 62:61-69.

- Fanning, D.S. and Keramidas, V.Z. 1977. Micas. Pages 195-258. In J.B. Dixon and S.B. Weed, (eds.) Minerals in soil environments. Soil Sci. Soc. Am. Madison WI.
- Fraleigh, J.B. 1985. Calculus with analytical geometry. 2nd edition, pg. 210-215, Addison-Wesley, Reading, Mass.
- Genrich, D.A. and Bremner, J.W. 1972. A reevaluation of the ultrasonic vibration method of dispersing soils. Soil Sci. Soc. Am. Proc. 36:944-947.
- Goss, C.J. 1987. The kinetics and reaction mechanism of the goethite to hematite transformation. Mineral. Mag. 51:437-451.
- Jackson, M.L. 1979. Soil chemical analysis--Advanced course. 2nd Ed., 11th printing. Published by the author, Madison WI.
- Kerr, P.F., Hamilton, P.K., Pill, R.J., Wheeler, G.V., Lewis, D.R., Burkhardt, W., Reno, D., Taylor, G.L., La Habra Laboratory, Mielenz, R.C., King, M.E., and Schieltz, N.C. 1950. Analytical data on reference clay minerals. American Petroleum Institute. Project 49, Clay Mineral Standards, Preliminary report #7. Columbia University, New York. 160pp.
- Kodama, H. 1979. Clay minerals in Canadian soils: Their origin, distribution and alteration. Can. J. Soil Sci. 59:37-58.
- Lindsay, W.L. 1979. Chemical equilibria in soils. John Wiley & Sons, New York, Pg. 284.
- Lipman, J.G. Waksman, S.A., and Joffe, J.S. 1921. The oxidation of sulfur by soil microorganisms. Soil Sci. 12:475-489.
- Mehra, O.P. and Jackson, M.L. 1959. Constancy of the sum of mica unit cell potassium surface and interlayer sorption surface in vermiculite-illite clays. Soil Sci. Soc. Am. Proc. 23:101-105.
- Mehra, O.P. and Jackson, M.L. 1960. Iron oxide removal from soils and clays by a dithionite-citrate system buffered with sodium bicarbonate. Clays and Clay Minerals 7:317-327.
- McKeague, J.A. and Day, J.H. 1966. Dithionite- and oxalate-extractable Fe and Al as aids in differentiating various classes of soils. Can. J. Soil Sci. 46:13-22.
- McKeague, J.A. 1967. An evaluation of 0.1 M pyrophosphate and pyrophosphate-dithionite in comparison with oxalate as extractants of the accumulation products in podzols and some other soils. Can. J. Soil Sci. 47:95-99.
- McKeague, J.A. (ed.) 1978. Manual on soil sampling and methods of analysis. 2nd Edition. Can. Soc. Soil Sci. Subcommittee on methods of analysis.
- McLean, H.C. 1918. The oxidation of sulfur by microorganisms in its relation to the availability of phosphates. Soil Sci. 5:251-290.
- Parfitt, R.L., and Kimble, J.M. 1989. Conditions for formation of allophane in soils. Soil Sci. Soc. Am. J. 53:971-977.
- Pawluk, S. 1971. Characteristics of Fera Eluviated Gleysols developed from acid shales in northwestern Alberta. Can. J. Soil Sci. 51:113-124.

- Ross, G.J. 1969. Acid dissolution of chlorites: Release of magnesium, iron and aluminum and mode of acid attack. *Clays and Clay Minerals* 17:347-354.
- Ross, G.J. and Kodama, H. 1973. Experimental transformation of a chlorite into a vermiculite. *Clays and Clay Mins.* 22:205-211.
- Roy, A.B. and Trudinger, P.A. 1970. *The biochemistry of inorganic compounds of sulphur.* Cambridge University Press, New York. 400 pp.
- Schwertmann U. and Murad, E. 1983. Effect of pH on the formation of goethite and hematite from ferrihydrite. *Clays and Clay Mins.* 31:277-284.
- Senkayi, A.L., Dixon, J.B. and Hossner, L.R. 1981. Transformation of chlorite to smectite through regularly interstratified intermediates. *Soil Sci. Soc. Am. J.* 45:650-656.
- Theisen, A.A. and Harward, M.E. 1962. A paste method for preparation of slides for clay mineral identification by X-ray diffraction. *Soil Sci. Soc. Am. Proc.* 26:90-91.
- Younge, O.R. 1931. Sulphur oxidation and reaction effects in Alberta soils. *Sci. Agric.* 9:535-541.

3. ACIDIFICATION ADJACENT TO AN ELEMENTAL SULFUR STOCKPILE: II TRACE ELEMENT REDISTRIBUTION¹

3.1 INTRODUCTION

Elemental sulfur is produced through the removal of H_2S from sour natural gas and is a major by-product of the petroleum and gas industry. Sulfur recovered during the processing of sour natural gas has traditionally been stockpiled on gas plant sites in the form of large blocks covering areas of up to several hectares. A sulfur block may exist for several decades before it is dismantled. During this period some sulfur escapes, usually in the form of finely divided wind blown particles or larger fragments that dislodge from the vertical sides of the stockpile. The liberated sulfur is deposited on soil in the vicinity of the block with the greatest amounts accumulating in the immediately vicinity, decreasing with distance away from the site. Elemental sulfur quickly oxidizes to H_2SO_4 in aerobic soil environments. The pH value of soil contaminated with elemental sulfur may decrease to below 2.0 depending on the amount of sulfur deposited on a local area and the buffering capacity of the soil.

Mineral soil material contains a variety of trace elements that are released very slowly during the natural weathering of soil. The amount of mobilization and translocation of trace elements in Canadian soils is usually minimal because of the recent origin of these soils (McKeague et al. 1979; McKeague and Wolynetz 1980). The solubilities of most metals greatly increase with increasing acidity. Background levels of many trace elements, particularly the first row transition elements, As, Pb, Sr, and Hg, have been documented for many noncontaminated soils of the Interior Plains (Mills and Zwarich 1975; Dudas and Pawluk 1976; 1977; McKeague et al. 1979; Dudas and Pawluk 1980; McKeague and Wolynetz 1980; Spiers et al. 1989). Few studies have included values for the rare earth elements.

It was recently demonstrated that some soil minerals are selectively altered, dissolved, and formed under the extremely acid conditions generated adjacent to stockpiles of elemental sulfur (Chapter 2). Minerals that were totally or partially dissolved included Fe-rich primary minerals,

¹A version of this chapter has been submitted for publication. C.J. Warren and M.J. Dudas. 1991. Can. J. Soil Sci.

chlorite, plagioclase feldspars, carbonates, and smectite. The fractionation of trace elements among soil minerals and their translocation in extremely acidic soil adjacent to elemental sulfur blocks have not previously been examined in detail. Trace elements concentrated in these mineral phases or adsorbed onto particle surfaces may be released at concentrations much higher than under natural weathering conditions. Therefore, the potential exists for the contamination of groundwater through the mobilization and transport of some trace elements associated with soil mineral phases. Knowledge of elemental removal from acidified material may also be useful in plant nutrition aspects of reclaiming sulfur block sites.

The objective for this chapter was to determine the total content and examine the redistribution of trace elements within surficial till material influenced by extreme acidity resulting from the oxidation of elemental sulfur adjacent to an elemental sulfur block. Samples obtained for mineralogical study (Chapter 2) were used in the current study on trace elements. The possibility of metal loading in association with the addition of elemental sulfur was also considered. Data on background levels are presented for some trace elements not previously documented for soils of the Interior Plains.

3.2 MATERIALS AND METHODS

Samples of surficial materials were collected from around a sulfur stockpile located about 3 km south of the townsite of Olds, Alberta in SE 1/4, section 18, township 32, range 1 west of the fifth meridian. The sulfur block was 25 years old, about 10 m high, and covered over 10,000 m² at the time of sampling. The surficial geological material in the area was a calcareous till of continental origin. Prior to construction of the stockpile the soil solum had been stripped from the site and the sulfur block had been erected directly on the underlying calcareous till.

Four replicate sampling pits up to one meter deep were excavated at spacings of 5 m along the west side of the block starting 10 m from the NW corner. All pits were located within two meters of the side of the block. Samples were collected in each pit from a cross sectional exposure orientated parallel to the vertical face of the block. Samples representing 5 cm depth increments were collected to a depth of 75 cm. Four replicate samples of the unaltered calcareous till were also collected at 5 m

spacings along a recently exposed embankment located about 50 m west of the block. The characteristics of the till at these sites were considered to be those of the calcareous parent material of the soil prior to any chemical alteration derived from the effects of the sulfur block. All samples were air dried and ground to pass a 2 mm sieve. A detailed description of soil materials is provided in Chapter 2 (Table 2.1).

Approximately one gram subsamples of the bulk soil from selected 5 cm depth increments from three of the pits and triplicate powdered samples of elemental sulfur obtained from the side of the block were submitted to Nuclear Activation Services Ltd. (McMaster University, Hamilton, Ontario, Canada) to determine total concentrations of Ag, As, Ba, Co, Cr, Cs, Ga, Hf, Mn, Mo, Ni, Rb, Sb, Sc, Se, Sr, Ta, Th, U, V, W, Zn, La, Ce, Nd, Sm, Eu, Gd, Tb, Dy, Yb, and Lu, by instrumental neutron activation analysis (INAA). The total concentration of boron was determined by neutron activation prompt- γ analysis using the same samples. To determine total content of Hg, triplicate subsamples of the soil materials and elemental sulfur were digested with HNO_3 and the digests analyzed by cold vapor atomic absorption spectrophotometry (Melton et al. 1971; Dudas and Pawluk 1976).

3.3 RESULTS

The profile adjacent to the sulfur block consisted of three distinct layers. Material at the surface to a depth of about 45 cm was extremely acid with pH values ranging between 1.6 and 2.9. Discrete nodules of gypsum ($\text{CaSO}_4 \cdot 2\text{H}_2\text{O}$) were observed within the acidified surface material. Directly underlying the acidic surface material was a reddish colored indurated layer about 10 to 15 cm thick. The layer was enriched in Fe, displayed a coarse platy structure, and ranged in pH value from 3.8 at the top to 6.6 at the bottom. Beginning at the top of the indurated layer, carbonate contents increased with depth to a maximum of $120 \text{ g} \cdot \text{kg}^{-1} \text{ CaCO}_3$ equivalent below 65 cm depth. The pH values of soil below 65 cm depth ranged between 7.0 and 8.0. Detailed characteristics of the profile and mineralogical composition of the soil materials from each depth range are described elsewhere (Chapter 2).

Trace element translocation in soil material can be assessed through the analysis of solid weathered residues (Koons et al. 1980; Warren and Dudas 1988). The technique of instrumental neutron activation analysis (Ehmann and Vance 1989) is a very sensitive method for determining the concentration of a wide range of trace elements in a single soil sample. Analysis of weathered residues provides the ability to detect changes in the content of many trace elements at very low concentrations. The technique also allows assessment of attenuation of elements by the weathered residues.

The content of trace elements determined in the elemental sulfur and in samples from selected depths within the soil profile are given in Table 3.1. The total concentrations of Ag, Mo, Ni, Se, and W in all samples were below the detection limits for INAA (0.2, 0.4, 50, 0.5, and 1 mg·kg⁻¹, respectively). The sulfur contained detectable amounts of B, Cr, Mn, and U at concentrations far less than the contents of the soil material. The concentrations of all other trace elements in the elemental sulfur were below detection limits for INAA. The concentrations of all trace elements determined in the soil material were within the average range for soils and lithospheric concentrations (Taylor 1964; Bowen 1979). Concentrations were also comparable with those reported by others for soil parent materials of the Interior Plains (McKeague and Kloosterman 1974; Mills and Zwarich 1975; Dudas and Pawluk 1976; McKeague et al. 1979; Dudas and Pawluk 1980; McKeague and Wolynetz 1980; Spiers et al. 1989).

The concentrations of ten of the 14 naturally occurring lanthanides in the profile were slightly lower than values reported by Bowen (1979) for average soil concentrations (Table 3.2). The concentrations of all lanthanides in the elemental sulfur were below the detection limits for INAA. All lanthanides were depleted slightly in the acidified material and were not enriched in the underlying calcareous material relative to the content of the parent material sample obtained 50 m from the site of the block.

Table 3.1 Concentration of trace elements in bulk samples from selected depths. Values in brackets indicate detection limits for each element. Values for elemental concentration for each depth followed by the same letter are not significantly different ($P = 0.95$, Tukey's HSD interval, $n=3$).

Depth (cm)	As	B	Ba	Co	Cr	Cs	Ga	Hf	Hg
	(0.2)	(0.2)	(20)	(0.1)	(0.2)	(0.1)	(5)	(0.1)	(0.1)
S^0	<0.2	0.7	<20	<0.1	0.4	<0.1	<5	<0.1	<0.1
0-5	1.8 b	40 ab	630 a	1.3 b	36 a	2.5 ab	7 c	4.5 a	15 b
20-25	2.1 b	39 ab	600 a	1.3 b	32 a	2.6 ab	7 c	3.8 ab	40 a
40-45	6.2 ab	37 ab	610 a	2.2 ab	33 a	2.3 ab	8 c	3.7 ab	40 a
45-50	9.2 a	30 b	440 b	12 a	42 a	1.9 b	25 a	2.9 b	41 a
60-65	8.2 a	44 a	560 ab	9.9 ab	46 a	3.3 ab	19 ab	3.3 b	59 a
70-75	6.0 ab	45 a	600 a	7.5 ab	47 a	3.6 a	9 bc	3.3 b	51 a
Parent Till	4.9 ab	39 ab	560 ab	6.0 ab	37 a	2.1 ab	17 b	3.5 ab	44 a
Soil Ave. **	6	20	500	8	70	4	20	3	60

	Mn	Rb	Sb	Sc	Sr	Ta	Th	U	V	Zn
	(0.1)	(5)	(0.1)	(0.05)	(50)	(0.1)	(0.1)	(0.01)	(0.5)	(3)
S^0	1	<5	<0.1	<0.05	<50	<0.1	<0.1	0.02	<0.5	<3
0-5	36 b	53 a	0.9 a	4.4 b	50 a	0.5 a	3.4 c	1.7 b	75 a	12 b
20-25	40 b	62 a	0.8 a	4.7 b	97 a	0.6 a	3.3 c	1.6 b	53 a	21 b
40-45	59 b	56 a	0.7 a	4.4 b	140 a	0.4 a	4.0 bc	1.7 b	76 a	22 b
45-50	400 a	58 a	0.7 a	7.4 a	50 a	0.4 a	7.8 a	2.2 ab	72 a	59 a
60-65	440 a	84 a	1.1 a	8.2 a	73 a	0.6 a	7.0 a	2.8 a	95 a	92 a
70-75	470 a	70 a	1.0 a	8.0 a	50 a	0.5 a	7.1 a	2.6 a	88 a	84 a
Parent Till	360 a	54 a	1.0 a	5.7 ab	90 a	0.4 a	6.1 ab	2.7 a	86 a	46 a
Soil Ave. *	1000	150	1	7	250	2	9	2	90	90

* Values from Bowen, 1979

Table 3.2 Concentration of lanthanides in the bulk samples from selected depths in the profile.

Values in brackets indicates INAA detection limits for each element. Values for elemental concentration for each depth followed by the same letter are not significantly different ($P = 0.95$, Tukey's HSD interval, $n=3$).

Depth	La	Ce	Nd	Sm	Eu	Gd	Tb	Dy	Yb	Lu
	(0.1)	(0.5)	(0.5)	(0.05)	(0.05)	(0.5)	(0.05)	(0.5)	(0.01)	(0.01)
0-5	17.1 b	27.0 b	9.7 c	1.61 c	0.40 b	1.2 c	0.21 b	1.7 b	1.14 cd	0.20 cd
20-25	18.1 b	28.5 b	10.4 bc	1.74 c	0.40 b	1.0 c	0.41 ab	1.8 b	0.98 d	0.18 d
40-45	17.8 b	27.1 b	11.7 bc	1.76 c	0.36 b	0.9 c	0.39 ab	1.6 b	1.00 d	0.18 d
45-50	24.7 a	43.0 a	17.7 a	4.04 a	0.93 a	3.7 a	0.69 a	4.7 a	1.74 a	0.30 a
60-65	26.7 a	45.3 a	17.3 a	4.01 a	0.83 a	3.5 ab	0.65 a	4.2 a	1.77 a	0.30 a
70-75	25.1 a	42.0 a	15.6 ab	3.61 a	0.84 a	3.0 ab	0.64 a	3.5 a	1.62 ab	0.28 ab
Parent Till	23.5 a	38.1 a	14.7 abc	2.86 b	0.54 b	2.5 b	0.69 a	3.6 a	1.39 bc	0.24 bc
Soil* Ave.	40	50	35	4.5	1.0	4.0	0.7	5.0	3.0	0.40

*Values from Bowen, 1979

Translocation of trace elements within the sampled profile followed three general patterns. The first group of elements were those depleted in the acidified material (0 to 45 cm depth range) relative to the underlying calcareous parent material (60 to 75 cm depth range). This group included As, Co, Ga, Mn, Sc, Th, U, Zn, and the lanthanides. The elements As, Co, and Ga accumulated in the Fe-rich layer (45-50 cm depth). Accumulations of Mn, Sc, Th, U, Zn, and the lanthanides were not observed in the sampled profile. The second group of elements included only Ba and Hf which were enriched in the surface acidified material relative to the calcareous parent material. The third group of elements were those displaying little difference in concentrations between the acidified and calcareous materials. This group included B, Cr, Cs, Hg, Rb, Sb, Sr, Ta, and V. The content of all trace elements in parent till sampled 50 m from the block were not significantly different ($P < 0.95$) from the trace element content of the calcareous materials underlying the acidified layer (Table 3.1).

trace elements in parent till sampled 50 m from the block were not significantly different ($P < 0.95$) from the trace element content of the calcareous materials underlying the acidified layer (Table 3.1).

3.4 DISCUSSION

Dissolution and translocation of trace elements within the soil material adjacent to the elemental sulfur block was interpreted within the context of dissolution and precipitation of mineral phases (Chapter 2). Primary Fe-containing minerals, carbonates, chlorite, and plagioclase feldspars were the least resistant to dissolution in the acidified material. Potassium feldspars, muscovite, kaolinite, and quartz were residual. The Fe-rich indurated layer that formed between the acidic and calcareous layers contained secondary Fe-oxyhydroxides that could act to adsorb or coprecipitate some trace elements. The impervious nature of the layer also acted to deflect flow of solutes in the acidified material under the stockpile (Chapter 2).

The elemental sulfur from the stockpile contained concentrations of trace elements far below total concentrations in the soil (Table 3.1) and therefore was responsible for nearly negligible additions of trace elements to the soil. The elements mobilized within the affected soil material were strictly those native to the parent material.

Elements that were dissolved and mobilized were those commonly associated with minerals preferentially dissolved under acidic conditions. The elements As, Co, and Ga displayed the greatest amount of translocation within the influenced soil material. The concentrations of these three elements were reduced in the surface layers of the acidified material by at least 50% compared to the calcareous parent material (Table 3.1). Cobalt and As are commonly associated with Fe-containing primary minerals such as pyroxenes and amphiboles. Gallium commonly substitutes for Al in aluminosilicates such as feldspars and phyllosilicates (Levinson 1980; Kabata-Pendias and Pendias 1984). Dissolution of these minerals along with exchangeable and adsorbed forms of the elements would account for depletion of the elements from the acidified material. Cobalt, As, and Ga were also enriched in the Fe-rich layer relative to the calcareous material (Table 3.1) suggesting attenuation by the Fe oxyhydroxides or precipitation by mechanisms similar to those of Fe (Koons et al. 1980).

The contents of Mn, Sc, and Zn were also significantly reduced in the acidified surface material but were not enriched in the Fe-rich layer. Manganese and Zn are usually associated with Fe bearing primary minerals and with the clay fraction of soils as structural, adsorbed, and exchangeable cations. Scandium commonly substitutes for Al^{3+} , Fe^{3+} and Ti^{4+} in ferromagnesian minerals and biotite (Kabata-Pendias and Pendias 1984). Removal of Mn, Sc, and Zn from the acidified material followed depletion of Fe bearing primary minerals at the present site. Removal of more than 85% of the total Mn from the acidified material further suggested that the phyllosilicates dissolved from the acidified soil material also contained Mn. Lack of enrichment in the Fe-rich layer suggested little attenuation of Mn by the newly precipitated Fe phases. Attenuation by free Fe oxides has been observed for Mn, Sc, and Zn in other weathered soil materials (Koons et al. 1980). Manganese, Zn, and Sc form strong neutral charged aqueous complexes with sulfate. Formation constants for the aqueous sulfate complexes are in the order of 10^2 (Lindsay 1979). Formation of neutral aqueous sulfate complexes would inhibit both precipitation with Fe and adsorption by the secondary Fe-minerals. Enrichment was also not apparent in the carbonate material underlying the acidified layer further indicating that the formation of neutral sulfate complexes may have prevented attenuation of Mn, Zn, and Sc by the carbonate material and/or that the elements were dissolved after the development of the indurated layer and thus their movement as solutes was diverted under the stockpile.

Mercury displayed unique behavior among the trace elements. The abundance of Hg in C horizon material is usually greater than in A horizons. The content of Hg in the samples at the present site was similar to values reported for C horizons of other soils from southern Alberta (Dudas and Pawluk 1976). Reduction in the content of Hg was significant only in the zero to five cm layer (Table 3.1). The content of Hg in layers deeper in the profile were not significantly different. Loss of Hg only from the surface layer suggested that Hg was lost due to volatilization from the soil surface to the atmosphere (Dudas and Pawluk 1976) and not through leaching.

The two naturally occurring actinides, U and Th, are usually associated with the clay fraction of soils (Harmsen and de Haan 1980). The Th/U ratio in all samples was below the expected value of 3 for lithospheric materials. The concentration of Th in the parent material was slightly lower than the

value of 9.0 reported by Bowen (1979). This suggested that Th was preferential leached from the material compared to U. Reduction in the contents of chlorite and smectite from the acidified soil material (Chapter 2) suggested that Th and U were more closely associated with chlorite and smectite in the parent material than muscovite or kaolinite.

Thorium and U were not enriched in the Fe-rich (45-50 cm depth) layer and no significant differences were observed in the Th and U contents of the calcareous material below 45 cm depth and the unaffected parent material (Table 3.2). Thorium and U were dissolved in a sulfate rich medium at low pH and translocated downward within the profile into environments with higher pH values. Thorium and U react in aqueous solution to form hydrous oxides and hydroxide species (Ryan and Rai 1983; 1987). At pH values greater than about 4.0 the dominant aqueous species are the non-charged hydroxides (Baes and Mesmer 1976). Formation of neutral charged sulfate complexes of U and Th are also possible (Wallace 1967). Formation of non-charged aqueous species of Th and U within the profile would inhibit adsorption and retention within the profile.

All of the lanthanides displayed similar behavior within the acidified material (Table 3.2). Between 30 and 50% of the total amount of each lanthanide was removed from the acidified surface layers. Dissolution of the lanthanide elements in similar ratios indicated similar distributions among the minerals dissolved under acidic conditions. The lanthanides were not significantly enriched in the Fe-rich or the calcareous material. The lanthanide elements are all large (>84 pm) usually trivalent cations that do not hydrolyze significantly at pH values less than 6.0 (Baes and Mesmer 1976). The lanthanides form strong mono- and di-sulfate complexes (Wood 1990) which are not strongly adsorbed by charged surfaces thus accounting for the lack of attenuation in the subsurface layers.

Only Ba and Hf were enriched in the acidified material and similar to Si and Na. The solubility of Ba in this system was controlled by barite (BaSO_4). The solubility product for the formation of barite (Stumm and Morgan 1981) heavily favours precipitation of the solid. The great abundance of sulfate in the surface layer would therefore reduce the solution levels of Ba to very low levels and inhibit leaching of the element. Although Sr was not enriched in the acidified material, formation of insoluble sulfates may have similarly inhibit translocation within the soil material.

Hafnium commonly substitutes for Si in most silicate minerals (Kabata-Pendias and Pendias 1984) and therefore would be retained similar to Si in the residue material (Chapter 2).

Elements that showed no significant translocation within the profile were likely associated with mineral phases resistant to acid weathering. Most of the B in the samples was likely associated with weather resistant tourmaline ($\text{Na}(\text{Mg,Fe})_3\text{Al}_6(\text{BO}_3)_3(\text{Si}_6\text{O}_{18})\text{OH}$) or primary muscovite (Harder 1961; Kantor and Schwertmann 1974) which was residual in the profile. Rubidium and Cs were also not translocated significantly within the sampled profile (Table 3.1). Rubidium and Cs commonly substitute for K in muscovite and/or potassium feldspars which were minimally or not dissolved from the acidic material (Chapter 2). Vanadium and Sb are usually considered mobile elements in soil but displayed no significant differences in concentration with depth. Chromium commonly occurs in soil as the weather resistant mineral chromite (FeCr_2O_4) and substitutes for Fe and Al in phyllosilicates. Lack of mobility of these elements suggested association with the minimally attacked phyllosilicates: kaolinite, and muscovite. The immobility of Ta may be explained by its sparingly soluble nature and/or association with muscovite in the profile (Levinson 1980).

In conclusion, trace elements mobilized within the soil material adjacent to the elemental sulfur stockpile were derived from mineral phases in the parent geological material that were selectively dissolved under extremely acidic conditions. Elemental sulfur did not contain trace elements in higher concentrations than the soil and therefore did not contribute significantly to contamination. The total concentrations of most trace elements were within the ranges reported for parent materials of other soils of the Interior Plains. The concentration of lanthanide elements at this site were generally lower than average lithospheric and soil concentrations. Most trace elements were redistributed within the sampled profile. Once the Fe-rich layer formed within the profile, it acted as a scavenger for As, Co, and Ga. The layer may have also diverted dissolved elements under the stockpile with the flow of water. Manganese, Sc, Th, U, Zn and the lanthanides were leached and removed from the sampled profile. Formation of aqueous sulfate complexes likely inhibited the attenuation of Mn, Sc, Zn, and the lanthanides. Barium and Hf were enriched in the acidified material while B, Rb, Cs, Sb, Sr, Br, Ta, and

V displayed no evidence of translocation within the profile. Mercury displayed the unique behavior of volatilization to the atmosphere from the soil surface.

3.5 REFERENCES

- Baes, C.F. and Mesmer, R.E. 1976. The hydrolysis of cations. Krieger Pub. Co. Malabar, Florida, 489pp.
- Bowen, H.J.M. 1979. Environmental chemistry of the elements. Academic Press, London, 317pp.
- Ehmann, W.D. and Vance, D.E. 1989. Advances in neutron activation analysis. CRC Critical Reviews in Anal. Chem. 20:405-443.
- Dudas, M.J. and Pawluk, S. 1976. The nature of mercury in Chernozemic and Luvisolic soils in Alberta. Can. J. Soil Sci. 56:413-423.
- Dudas, M.J. and Pawluk, S. 1977. Heavy metals in cultivated soils and in cereal crops in Alberta. Can. J. Soil Sci. 57:329-339.
- Dudas, M.J. and Pawluk, S. 1980. Natural abundances and mineralogical partitioning of trace elements in selected Alberta soils. Can. J. Soil Sci. 60:763-771.
- Harder, H. 1961. Einbau von bor in detritische tonminerale: Experimente zur erklärung des borgehaltees toniger sedimente. Geochim. Cosmochim. Acta 21:284-294.
- Harmsen, K. and de Haan, F.A.M. 1980. Occurrence and behaviour of uranium and thorium in soil and water. Neth. J. Agric. Sci. 28:40-62.
- Kabata-Pendias, A. and Pendias, H. 1984. Trace elements in soils and plants. CRC Press Inc. Boca Raton, Florida, 315pp.
- Kantor, W. and Schwertmann, U. 1974. Mineralogy and genesis of clays in red-black soil toposequences on basic igneous rocks in Kenya. J. Soil Sci. 25:67-78.
- Koons, R.D., Helmke, P.A. and Jackson, M.L. 1980. Association of trace elements with iron oxides during rock weathering. Soil Sci. Soc. Am. Proc. 44:155-159.
- Lindsay, W.L. 1979. Chemical equilibria in soils. John Wiley & Sons, New York, Pg. 284.
- Levinson, A.A. 1980. Introduction to exploration geochemistry. 2nd edition, Applied Pub. Ltd., Wilmette, IL 924pp.
- McKeague, J.A. and Kloosterman, B. 1974. Mercury in horizons of some soil profiles in Canada. Can. J. Soil Sci. 54:503-507.
- McKeague, J.A., Desjardins, J.G. and Wolynetz, M.S. 1979. Minor elements in Canadian soils. Land Resource Research Institute Contribution No. LRRI 27. Research Branch, Agriculture Canada. Ottawa, 75pp.
- McKeague, J.A. and Wolynetz, M.S. 1980. Background levels of minor elements in some Canadian soils. Geoderma 24:299-307.

- Melton, J.R., Hoover, W.L. and Howard, P.A. 1971. The determination of mercury in soils by flameless atomic absorption. *Soil Sci. Soc. Am. Proc.* 35:850-851.
- Mills, J.G. and Zwarich, M.A. 1975. Heavy metal content of agricultural soils in Manitoba. *Can. J. Soil Sci.* 55:295-300.
- Ryan, J.L. and Rai, D. 1983. The solubility of uranium(IV) hydrous oxide in sodium hydroxide solutions under reducing conditions. *Polyhedron* 2:947-952.
- Ryan, J.L. and Rai, D. 1987. Thorium(IV) hydrous oxide solubility. *Inorg. Chem.* 26:4140-4142.
- Spiers, G.A., Dudas, M.J. and Turchenek, L.W. 1989. The chemical and mineralogical composition of soil parent materials in northeast Alberta. *Can. J. Soil Sci.* 69:721-737.
- Stumm, W. and Morgan, J.J. 1981. *Aqueous Chemistry: An introduction emphasizing chemical equilibria in natural waters.* 2nd edition, Wiley, NY.
- Taylor, S.R. 1964. Abundance of chemical elements in the continental crust: A new table. *Geochim. Cosmochim. Acta* 28:1273-1285.
- Wallace, R.M. 1967. Determination of stability constants by donnan membrane equilibrium: the uranyl sulfate complexes. *J. Phys. Chem.* 71:1271-1276.
- Warren, C.J. and Dudas, M.J. 1988. Leaching behaviour of selected trace elements in chemically weathered alkaline fly ash. *Sci. Total Environ.* 76:229-246.
- Wood, S.A. 1990. The aqueous geochemistry of the rare-earth elements and yttrium. I: Review of available low-temperature data for inorganic complexes and the inorganic REE speciation of natural waters. *Chem. Geol.* 82:159-186.

4. DYNAMICS OF SOIL SOLUTION CHEMISTRY DURING LABORATORY INCUBATION OF SOIL AT 25°C

4.1 INTRODUCTION

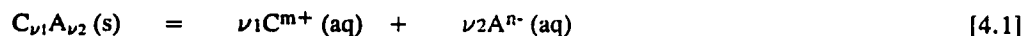
The soil solution may be described as the aqueous phase of the soil comprised of liquid water containing dissolved solids and gases. The chemical composition of the soil solution varies both spatially within the soil and with time as affected by temperature, interaction with solid and gaseous phases, evaporation and dilution (drying and wetting), and biological activity. As the soil solution is integral to most chemical reactions that occur in soil, characterization is fundamental to understanding soil chemical processes, particularly those involving mineral weathering.

Until recently, chemical characterization of the soil solution was tenuous because of difficulties associated with physical separation and isolation of representative samples of the aqueous phase from the soil matrix. Methods of extraction such as preparation of saturated pastes or 1:1 and 1:5 (soil:water) mixtures (e.g. Rhoades, 1982) circumvent this problem by increasing soil moisture contents to levels much higher than those generally observed under field conditions. It is commonly assumed that the concentration of dissolved species in saturation extracts are representative of the chemical composition of the soil solution (e.g. Beke and Palmer 1989) and that the resultant volume of added liquid equilibrates with solid phases within a very short period of time, usually within 48 h. These methods of sample preparation serve a practical purpose of providing routine methods of assessing and providing indices for soil properties of interest, such as salinity and acidity, but the extracts are not necessarily representative of the chemistry of the field soil water regime.

A major obstacle to extracting pore water from soils at moisture contents less than saturation is to overcome the extremely high tensions at which pore water is held within soil matrices. A variety of methods have been developed to extract samples of soil water and obtain sufficient volumes of solution for analysis. Methods of extraction include: drainage centrifugation (Gillman, 1976), miscible displacement using a second aqueous phase (Adams et al., 1980), vacuum displacement (Wolt and Gravelle 1986), and centrifugation with an immiscible organic liquid to displace the aqueous phase (Mubarak and Olsen, 1976; Whelan and Barrow, 1980). Use of these extraction methods coupled with

sensitive instrumental methods of analysis such as inductively coupled plasma atomic emission spectroscopy (ICP-AES), atomic absorption spectrophotometry, ion chromatography (IC), and instrumental neutron activation analysis, enable very detailed chemical characterization of the soil solution using only modest volumes of solution. The most promising technique for extraction of the soil solution for use in mineral stability studies is immiscible displacement (Mubarak and Olsen, 1976; Edmunds and Bath, 1976; Adams et al., 1980; Whelan and Barrow, 1980; Kittrick, 1980; 1983; Kinniburgh and Miles, 1983; Elkhatib et al., 1986). The method allows rapid extraction of pore water from soil samples ranging in texture from clay to sand and having moisture contents less than field capacity (moisture tensions greater than 33 kPa). In some studies the chemical composition of solutions extracted from different soils have been analyzed to compare different extraction methods (e.g. Adams et al., 1980; Whelan and Barrow, 1980), or mineral stability has been examined in simple systems (Kittrick, 1980; 1983). Few attempts have been made to examine mineral stability relationships in real soil systems.

The stability of minerals within a soil depend directly on the chemical composition of the aqueous phase. For a general precipitation-dissolution reaction (Sposito 1981):



the solubility product (K_{sp}) for the reaction is:

$$K_{sp} = (C^{m+})^{\nu_1} \cdot (A^{n-})^{\nu_2} / (C_{\nu 1}A_{\nu 2}) \quad [4.2]$$

where the activity of the solid ($C_{\nu 1}A_{\nu 2}$) is assumed to be unity for a pure phase. The ion activity product (IAP) for the solid is defined:

$$IAP = (C^{m+})^{\nu_1} \cdot (A^{n-})^{\nu_2} \quad [4.3]$$

where (C^{m+}) and (A^{n-}) represent the activities of component cations and anions, respectively, in the soil solution and ν_1 and ν_2 are the stoichiometric coefficients for the reaction. If the solid phase is in equilibrium with respect to the solution, then $IAP = K_{sp}$. If the solution is oversaturated with respect to the mineral, then $IAP > K_{sp}$, and in the case of undersaturation; $IAP < K_{sp}$.

Equilibrium is seldom, if ever, approached in soil because of environmental dynamics (e.g. fluctuating temperature and moisture conditions), the large number of competing reactions that occur in

soil, and differences in reaction rates (Furrer et al., 1989; Rai and Kittrick 1989). Alternatively, steady state conditions may be achieved whereby the concentration of dissolved solutes in the soil solution remain constant with time. Artificially controlling environmental variables such as temperature and soil moisture content at near constant values will eliminate the fluctuation in equilibrium relationships associated with temperature change and movement of solutes due to leaching. The composition of the soil solution from a soil maintained at constant temperature and moisture content should therefore reflect only the chemistries of competing reactions. The concentrations of solutes will approach some steady state level dependent on the total number of equilibrium relationships driving individual contributing reactions and the kinetics of the reactions. As a result, equilibrium thermodynamics can be meaningfully applied to solubility relationships of minerals in the system. The time required for the concentration of solutes to reach steady state levels in the soil pore water will depend on the relative reaction rates of competing reactions, the method of handling the sample, residence time of the pore water, and treatment of the sample prior to extraction of the pore water. The chemistries of the resulting equilibrated solutions may then be compared with calculated equilibria values to make estimates with respect to mineral stability and identify minerals important in controlling the concentration of solutes in solution.

The current study was initiated to determine the minimum sample incubation time required for the concentrations of soil solution solutes to approach steady state values. The first objective was to determine changes with respect to time in the concentrations and speciation of selected elements dissolved in the pore water of soil samples incubated in the laboratory at 25°C, ambient atmospheric pressure (1 atmosphere), and field capacity moisture content (33.3 kPa moisture tension). The second objective was to determine how the chemical composition of the soil solution is affected by sample pretreatment (i.e. air drying vs not drying). The values for temperature and pressure were chosen for the incubations because the vast majority of geochemical data are tabulated for these conditions. Field capacity moisture content was arbitrarily chosen to facilitate collection of sufficient volumes of solution for analysis.

4.2 MATERIALS AND METHODS

Samples used in this study were collected from a series of four replicate pits located along the side of a 25 year old elemental sulfur block as explained in detail in Chapter 2. The dominant soil in the area was an Orthic Black Chernozem (Udic Haploboroll) developed on late-Wisconsin calcareous till of continental origin. The soil solum had been stripped from the site and the sulfur block was constructed on what was initially calcareous till containing up to $190 \text{ g} \cdot \text{kg}^{-1} \text{ CaCO}_3$ equivalent (Chapter 2). Oxidation of elemental sulfur from the block in the surface material reduced pH values, ($2:1 \text{ mol} \cdot \text{dm}^{-3} \text{ CaCl}_2$) to approximately 2.0.

For the purposes of the current study, samples of two depths having greatly different pH values were chosen for the experiments. The first sample, identified here as the acidic sample, was from the 0 - 10 cm depth. The material had been strongly weathered through the oxidation of elemental sulfur, displayed soil pH values less than 2.0 in $0.01 \text{ mol} \cdot \text{dm}^{-3} \text{ CaCl}_2$, and contained an abundance of precipitated gypsum. The second sample, identified here as the calcareous sample, was obtained from the same profile at the 65 - 80 cm depth increment and displayed pH values between 7.3 and 7.6 in $0.01 \text{ mol} \cdot \text{dm}^{-3} \text{ CaCl}_2$.

Large bulk samples totaling approximately 45 kg were collected from the acidic and calcareous layers. Within 24 h of collection, samples were transported to the laboratory in their field moist state using large sealed plastic containers. On reaching the laboratory the samples from each depth were homogenized into single bulk samples that were later divided in half. One half was allowed to dry at ambient room temperature (air dry) and then passed through a 2 mm sieve as is commonly practiced in many soil laboratories. The other half was prevented from drying (identified here as non-dried), subdivided into smaller subsamples (described below), and the incubation period initiated immediately. Gravimetric moisture contents at matrix potentials of -33.3, -200, -400, -800, and -1500 kPa were determined for each sample depth by pressure plate extraction (McKeague, 1978) using aliquots of the air dried sieved samples.

The non-dried and re-wet air dried soils were incubated in approximately 250 g lots of moist soil (equivalent to approximately 190 to 200 g oven dry soil). All samples were incubated in 500 mL

plastic containers equipped with lids. A single hole (1 cm diameter) was punched in the center of each lid to allow aeration of the samples while preventing rapid and excessive evaporative of moisture. The air dried samples were placed into containers similar to the non-dried samples and re-wet by addition of deionized water. The mass of each sample was adjusted such that moisture tensions were equivalent to 33.3 kPa (field capacity). Sample masses were maintained at the calculated values for total mass throughout the incubation process by periodic additions of small amounts of deionized water. Fluctuations in sample mass due to addition and evaporation of water were not greater than 3 g (i.e. less than 2% of the total sample mass). Soil solutions were extracted from triplicate samples representing each depth and pretreatment after 1, 2, 4, 8, 16, 32, 64, and 128 days of incubation. Triplicate subsamples of the non-dried samples were also extracted prior to incubation. Pore water samples were obtained by centrifuging at a relative centrifugal force (RCF) of 37000 for one hour using tetrachloroethylene to displace the pore water (Whelan and Barrow, 1980; Elkhatab et al., 1986).

The pH values of the pore water extracts were determined immediately after collection. Samples of extracted soil solution were analyzed for total concentration of Al, Si, Fe, Ca, Mg, Na, K, and P by inductively coupled plasma atomic emission spectrophotometry (ICP-AES) and for total concentration of SO_4^{2-} by ion chromatography (IC). The concentrations of Cl^- , NO_3^- , and PO_4^{3-} in the extracts were very low compared to the concentration of SO_4^{2-} in the extracts and could not be determined by IC.

Elemental concentrations for the extracted solutions were used as input for the computer program MINTEQA2 (Felmy et al., 1984; Peterson et al., 1987; Brown and Allison, 1987). The program was used to calculate the speciation of 11 dissolved components (H^+ , Al, Si, Fe, Ca, Mg, Na, K, CO_3 , PO_4 , and SO_4) among 52 aqueous species including free ions, and sulfate, phosphate, hydroxide and carbonate ion pairs. Total P in the extracts as measured by ICP-AES was assumed to occur in solution as inorganic phosphate (PO_4). The partial pressure of gaseous CO_2 was assumed constant and equal to ambient atmospheric concentrations 3.2×10^{-2} kPa ($10^{-3.5}$ atmosphere). Redox potentials used in the calculations were assumed from Eh values commonly observed for aerobic soils based on the measured pH values (Baas-Becking et al. 1960). The redox conditions were assumed to

control the partitioning of total Fe among Fe(II) and Fe(III) species (Longmire et al., 1990). The saturation indices (SI) for selected mineral phases were also calculated with respect to the composition of speciated aqueous solution at each extract day.

4.3 RESULTS AND DISCUSSION

The mineralogy of the surficial till material at the site was previously characterized (Chapter 2) and was typical of soil parent materials from the Interior Plains region of western Canada (Pawluk 1961; Kodama 1979; Dudas and Pawluk 1982). Samples contained discrete kaolinite, dioctahedral mica, and smectite in the clay size (<0.002 mm) fraction. Chlorite was present in the parent calcareous material but absent in the acidified material. Primary minerals in the sand size fraction (2 - 0.05 mm diameter) of the calcareous sample included mostly quartz, with smaller amounts of alkali and potassium feldspars, and a small fraction composed of an assortment of higher density (density > 2.76 Mg·m⁻³) minerals. The primary minerals in the acidic sample were also dominated by quartz, but contained lesser amounts of the other primary minerals compared to the calcareous sample. The acidic sample contained large quantities of precipitated gypsum, whereas the calcareous sample contained an average equivalent CaCO₃ content of 100 g·kg⁻¹. Further details on the mineralogical and chemical characteristics of the samples at the site are described in Chapter 2.

The amount of moisture retained in the acidified material was higher than in the calcareous material at any given tension but the total amounts of solution extracted from each sample were similar (Figure 4.1). Moisture contents for all samples incubated at 33.3 kPa tension (field capacity) corresponding to 0.29 g·g⁻¹ for the acidic material and 0.25 g·g⁻¹ for the calcareous material. The amounts of solution extracted from both samples averaged 0.11 g·g⁻¹ and represented 38 and 44 % of the total mass of water in the acidic and calcareous samples, respectively. The consistent 4 to 5 % higher moisture contents observed for the acidic sample compared to the calcareous sample (Figure 4.1) was attributed to structural water associated primarily with gypsum (CaSO₄·2H₂O) which accumulated in the acidic material (Chapter 2). Gravimetric moisture contents (Θ_m) after extraction of pore water using the immiscible displacement technique were 0.18 g·g⁻¹ for the acidic sample and 0.14 g·g⁻¹ for

the calcareous sample which corresponded to matrix potentials of 920 and 1060 kPa, respectively (Figure 4.1).

The equivalent diameter of pores containing moisture after extraction by immiscible displacement was calculated using the equation of Hillel (1971) for capillary rise:

$$h_c = \frac{2 \cdot \gamma \cdot \cos \alpha}{r \cdot \rho_w \cdot g} \quad [4.4]$$

where h_c is the height of capillary rise, γ is the surface tension of water, α is the wetting angle of water (normally assumed equal to zero), r is the radius of the capillary, ρ_w is the density of water, and g is acceleration due to gravity. Using equation 4.4 it was calculated that any liquid water remaining in the samples after extraction using the immiscible displacement procedure was retained in pores with diameters of approximately 0.3 μm or less. Solutions were therefore extracted from large macropores, and soil pores associated with sand, silt, and coarse clay-sized particles but not necessarily from the pore space located between adjacent particles of fine clay (Diamond 1970).

The chemical composition of extracted pore water solutions have been shown to be independent of total moisture content for most soils (Kinniburgh and Miles, 1983). The solute content of extracts is not altered with extraction of increasing amounts of solution from samples with initial moisture contents below saturation (Edmunds and Bath 1976; Whelan and Barrow 1980; Elkhatab et al. 1986). It was therefore assumed for the current study that the chemistry of the bulk soil solution was homogeneous among all pores and the chemistry of the extracted pore water was representative of the bulk solution.

The pH values of the extracts from the air dried samples were consistently higher than the non-dried pretreatments for both the acidified and calcareous materials (Figure 4.2). The measured pH values of the solutions extracted from the non-dried acidified sample were initially 0.8 and increased to about 1.1 by the end of the 128 d incubation period. Values for the air dried samples were consistently about 0.3 to 0.4 pH units higher for the entire incubation period. The pH values of extracts from the

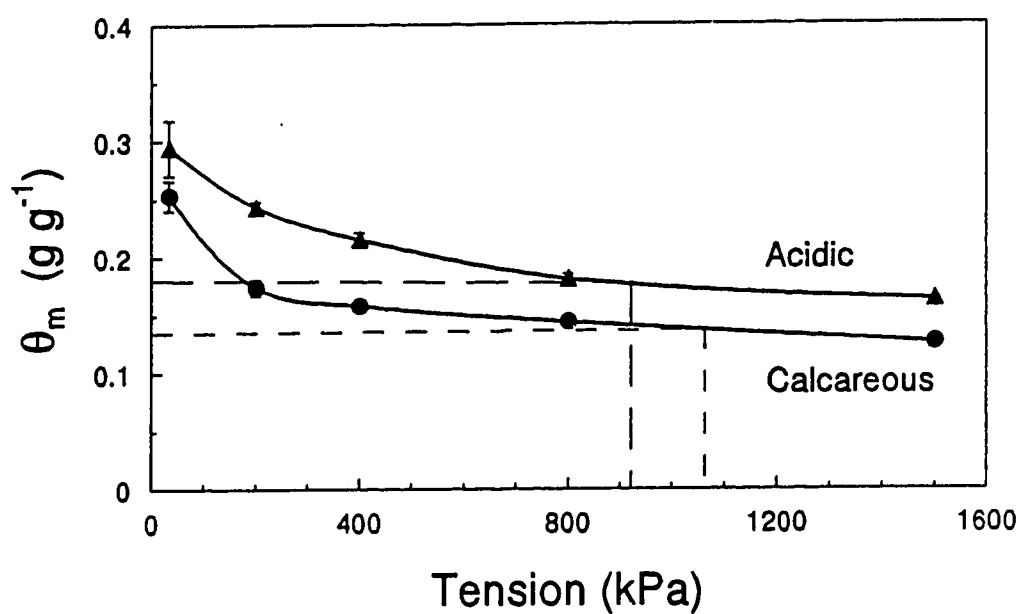


Figure 4.1 Moisture retention curves for the acidic and calcareous soil samples. Symbols indicate mean values ($n=3$) with standard deviations. Intersection of the dashed lines on each curve indicates the moisture contents and equivalent tensions after extraction by immiscible displacement.

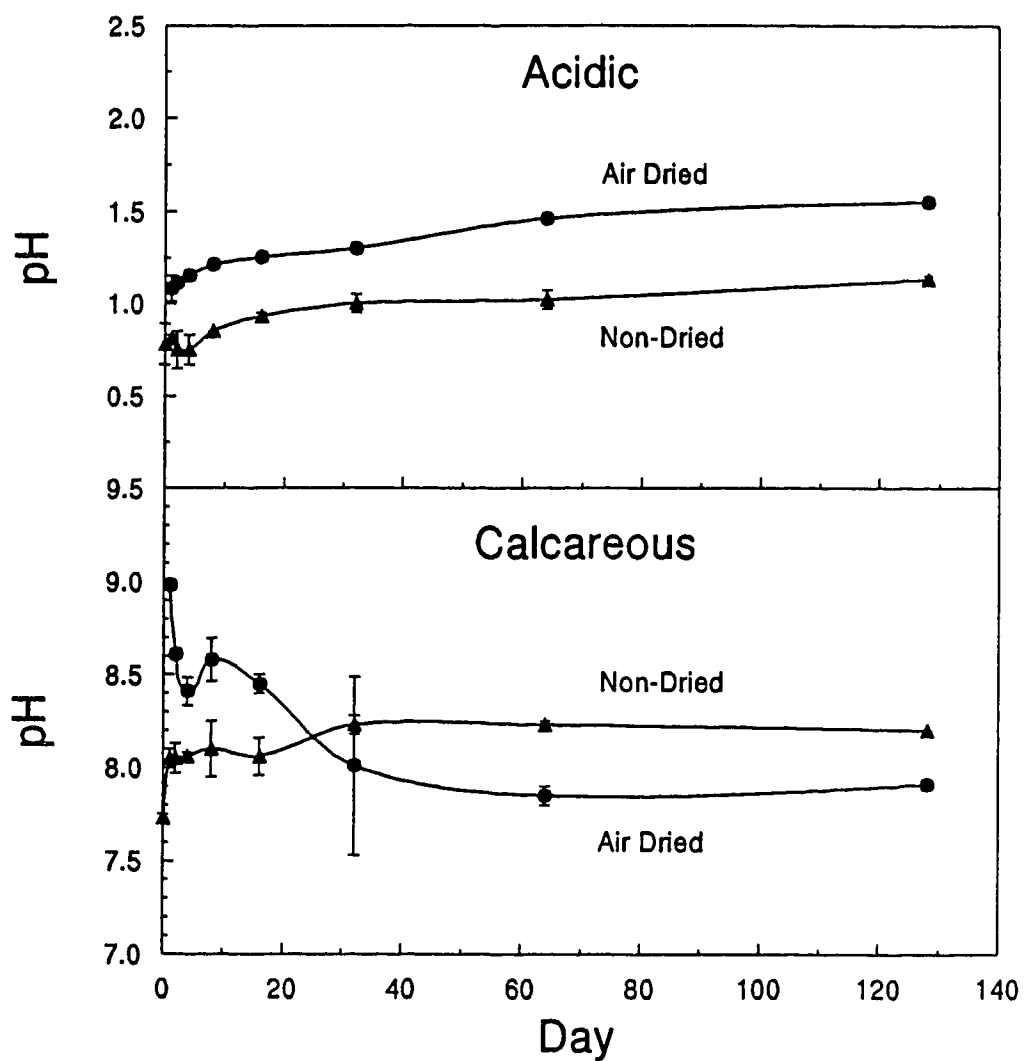


Figure 4.2 Measured pH values (with standard deviations) of the pore water extracted from the acidified and calcareous samples plotted against number of days after the start of incubation.

non-dried calcareous sample increased from an initial value of 7.7 on day 1 to between 8.0 and 8.2 where values were maintained for the remainder of the incubation period. The pH values for the air dried calcareous sample declined from an initial value of 9.0 to about 7.9 after 30 d of incubation.

The total concentrations of Al, Si, Fe, Ca, K, Mg, P, and SO₄ in the extracts as plotted against day of extraction after the start of incubation are presented in Figures 4.3 and 4.4. Concentrations in the extracts from the acidic layer were much higher than values observed for pore water extracted from the surface horizons of acidic soils (Simard et al. 1988; Qian and Wolt 1990). The concentrations of Al, Si, Fe, K, P, and SO₄ in the acidic material were 1 to 3 orders of magnitude higher than concentrations in the extracts from the calcareous samples. The concentrations of Ca and Mg in the acidic material was similar or slightly lower than concentrations in the calcareous material. Trends in the changes in concentration of Na in the extracts with respect to time (data not shown) were very similar to K. After some fluctuation during the first four days of incubation the concentrations of Si, P, and SO₄ in the non-dried samples of the acidic material and Al, Si, Ca, K, Mg, P, and SO₄ in the non-dried samples of the calcareous material remained nearly constant for the duration of the incubation period (Figures 4.3 and 4.4). The concentrations of Al, Fe, K, (Na), and Mg in the acidic material, increased at nearly constant rates during the entire 128 d incubation period.

The concentration of elements in the extracts from the air dried samples underwent large and sometimes abrupt changes during the first eight to 16 days of incubation compared to concentrations in the extracts from the non-dried samples (Figures 4.3 and 4.4). The concentrations of Al, Si, Fe, K, (Na), Mg, P, and SO₄ in the extracts from the air dried acidified material increased during the initial four days of incubation and then gradually decreased during the ensuing 12 d of incubation. After about 16 d of incubation concentrations tended to stabilize at slightly higher levels compared to levels for the non-dried samples. Increases with time in the pH values and near linear increases in the concentrations of Al, Fe, K, (Na), and Mg in the extracts from the non-dried acidic samples indicated that some soil minerals underwent dissolution at constant rates during the entire incubation period. Progressive increases in the pH values of the extracts with time indicated consumption of acid. Dissolution of soil minerals with time was indicated by the linear increases in the concentration of Al,

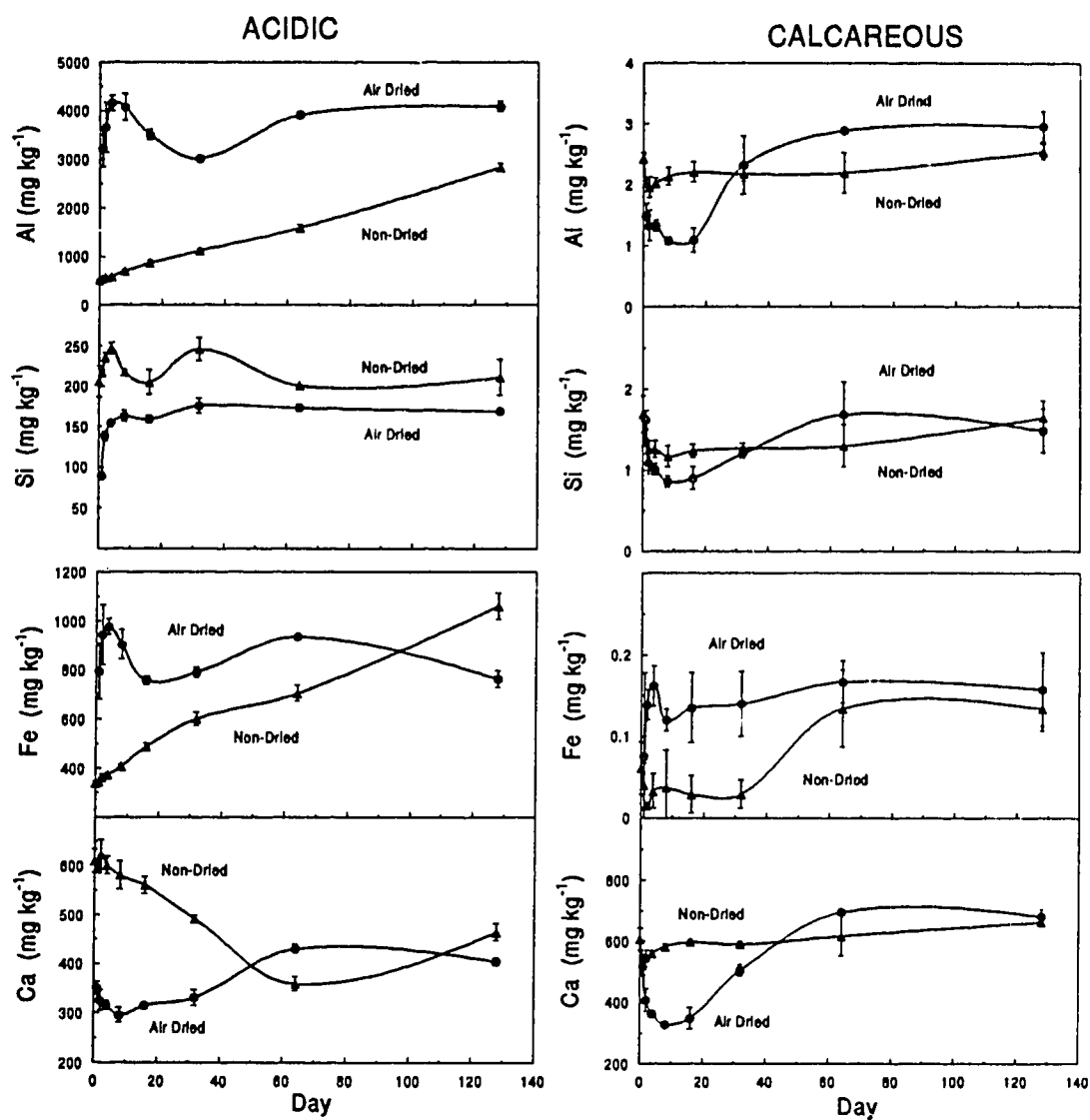


Figure 4.3 Mean concentrations (with standard deviations) of Al, Si, Fe, and Ca in the pore water samples extracted from the air dried and non-dried acidified and calcareous samples plotted against number of days after the start of incubation.

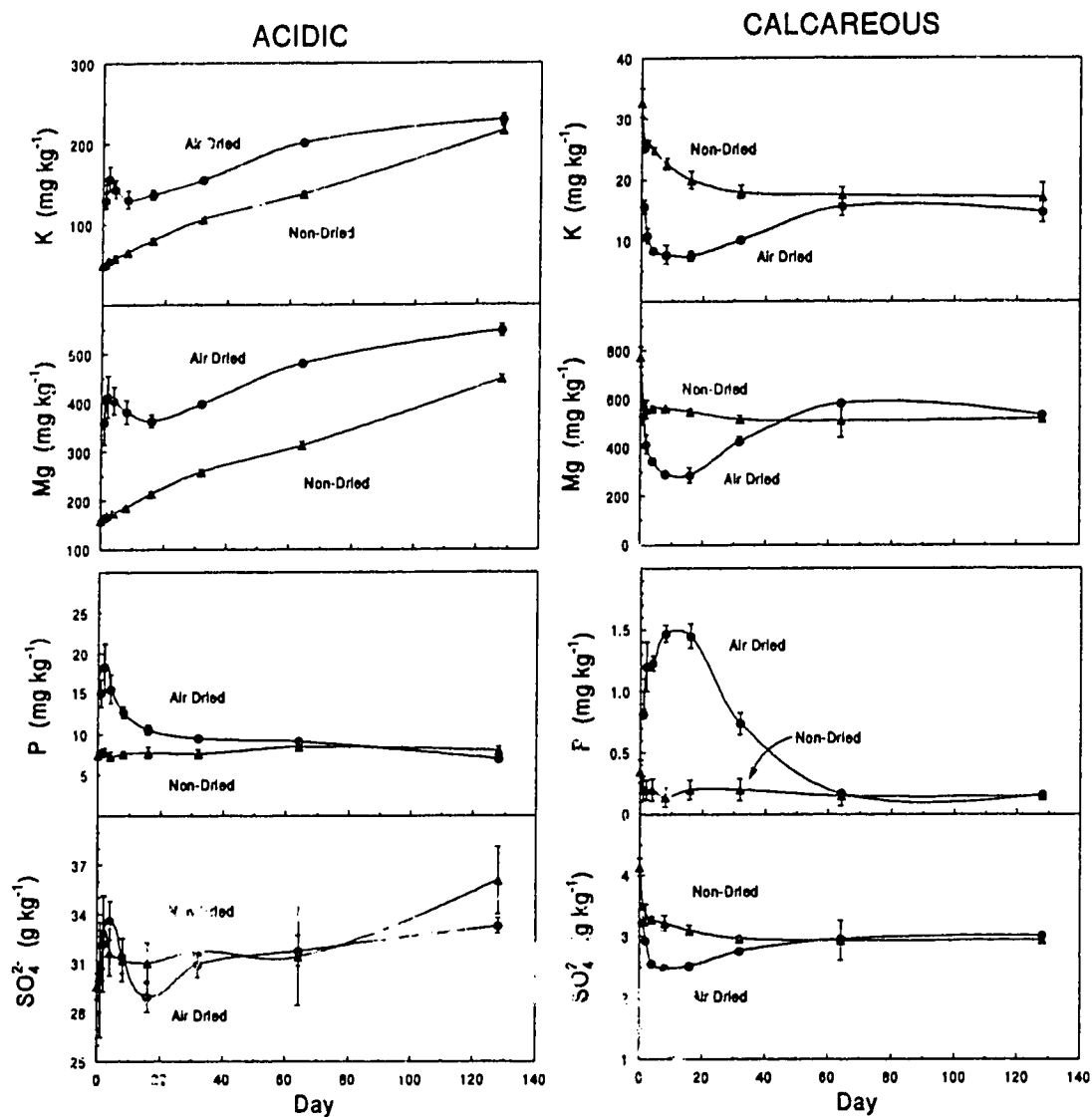


Figure 4.4 Mean concentrations (with standard deviations) of K, Mg, P, and SO_4 in the pore water samples extracted from the air dried and non-dried acidified and calcareous samples plotted against number of days after the start of incubation.

Fe, K, Mg, and Na which are major constituents of soil minerals such as feldspars and phyllosilicates. This is consistent with the observed decrease in the content of feldspars, chlorite, and heavy minerals in the acidic layer compared to the calcareous material (Chapter 2).

The concentration of elements in the extracts from the air dried acidic samples was usually slightly higher compared to the non-dried samples. Only the concentration of Si in the air dried acidic samples stabilized at lower concentrations compared to the non-dried material indicating that air drying altered the solubility controlling solids for Si possibly due to dehydration of amorphous Si. The concentrations of Ca in the initial extracts from the air dried acidic sample was lower than for the non-dried sample. The concentration of Ca in the air dried acidic sample increased while the concentration of Ca in the non-dried sample decreased with time. After approximately 50 d of incubation the level of Ca in the extracts was similar for both pretreatments for the duration of the incubation period.

Consistently higher pH values and higher concentrations of Al, Fe, K, Mg, and Na in the air dried acidic samples compared to the non-dried samples (Figures 4.2, 4.3, and 4.4) suggested that mineral dissolution was accentuated by the air drying process. Acid attack and dissolution of soil minerals was amplified during air drying in response to increasing the concentration of H_2SO_4 in the pore water facilitated by evaporation of water from the sample during the drying process. The high concentration of solutes formed on re-wetting the air dried samples suggested that elements dissolved from minerals during air drying formed efflorescent salts that rapidly re-dissolved on re-wetting. These were likely sulfate salts of the major elements precipitated reacting with the high concentrations of dissolved sulfate derived from H_2SO_4 . The concentration of elements in the extracted pore water observed after rewetting the air dried samples was therefore higher than concentrations in the non-dried samples.

The concentration of Al, Si, Ca, K, Mg, and SO_4 in the extracts from the air dried calcareous sample decreased during the first four to eight days of incubation and then increased gradually to concentrations similar to those obtained for the non-dried sample after about 40 to 60 d of incubation. The concentration of Fe in the air dried calcareous extracts was higher than the non-dried treatment but

values for the non-dried samples increased to similar levels after about 60 d of incubation. The concentration of total P in the extracts from the calcareous samples displayed trends similar to the acidic samples. Increases in the concentrations of P in the extracts from the air dried samples may have been due to increased phosphatase activity induced by a resurgence in biological activity on re-wetting (Spiers et al. 1979).

Decreases in the total concentrations of Al, Si, Ca, K, (Na), and SO_4 during the initial days of incubation after re-wetting of the air dried calcareous samples suggested the presence of precipitated secondary mineral phases. The high pH values of the extracts obtained for the first day of incubation suggested alkaline hydrolysis of minerals in the sample. Decreases in the concentrations may have been due to the formation of precipitates in response to the initially high pH values. The subsequent gradual increases in solute concentrations in the extracts from the air dried calcareous samples were likely in response to the decrease in pH values. Air drying the samples prior to incubation therefore perturbed the system resulting in solute concentrations not representative of the soil prior to sampling.

Only small differences were observed in the calculated distribution of aqueous species among total concentrations of the elements (Tables 4.1 and 4.2). Calculated percentage distributions of each component among aqueous species did not display large variations regardless of pretreatment, incubation period, or total solute concentrations. Most elements occurred in solution either as free ions or as sulfate complexes in the extracts from the acidic layer. Sulfate complexes also accounted for between 30 and 45% of the total Fe(II), Ca, and Mg in the extracts from the calcareous layer. The very high total concentration of sulfate in the soil solutions resulted in the formation of sulfate complexes which accounted for much larger percentages of most dissolved metals, compared to cultivated soils (e.g. Simard et al. 1988). The dominant sulfate species in the acidic sample was HSO_4^- , confirming a suggestion raised earlier in Chapter 2 that dissolved HSO_4^- constituted a large percentage of the total sulfate species in the acidic material. The calculated amount of HSO_4^- in solution tended to decrease with time as the concentrations of metals that form aqueous sulfate complexes increased in concentration.

Table 4.1 Percent distribution of components among aqueous species in the extracts from the air dried and non-dried acidic samples after 1 day and 128 days of incubation.

Component	Species	Non-dried		Air Dried	
		Day 1	Day 128	Day 1	Day 128
Al	Al^{3+}	43	28	38	25
	AlSO_4^+	31	31	31	30
	$\text{Al}(\text{SO}_4)_2^-$	26	41	30	44
Si	H_4SiO_4	100	100	100	100
Fe(II)	Fe^{2+}	70	60	67	58
	$\text{FeSO}_4 \text{ aq}$	30	40	33	42
Fe(III)	Fe^{3+}	11	7	9	6
	FeSO_4^+	63	58	57	55
	$\text{FeH}_2\text{PO}_4^{2+}$	5	5	12	7
	$\text{Fe}(\text{SO}_4)_2^-$	21	30	22	32
Ca	Ca^{2+}	67	57	64	54
	$\text{CaSO}_4 \text{ aq}$	33	43	36	46
Mg	Mg^{2+}	70	60	67	58
	$\text{MgSO}_4 \text{ aq}$	30	40	33	42
Na	Na^+	95	92	94	91
	NaSO_4^-	5	8	6	8
K	K^+	93	90	92	89
	KSO_4^-	7	10	8	11
PO_4	H_2PO_4^-	6	9	8	16
	$\text{H}_3\text{PO}_4 \text{ aq}$	85	56	62	39
	$\text{FeH}_2\text{PO}_4^+$	3	12	10	14
	$\text{FeH}_2\text{PO}_4^{2+}$	6	22	19	28
SO_4	SO_4^{2-}	14	18	16	21
	AlSO_4^+	2	9	12	13
	$\text{Al}(\text{SO}_4)_2^-$	3	23	23	39
	$\text{CaSO}_4 \text{ aq}$	2	1	1	1
	HSO_4^-	78	45	45	20
	$\text{MgSO}_4 \text{ aq}$	1	2	2	3
CO_3	$\text{H}_2\text{CO}_3 \text{ aq}$	100	100	100	100

Table 4.2 Percent distribution of components among aqueous species in the extracts from the air dried and non-dried calcareous samples after 1 day and 128 days of incubation.

Component	Species	Non-dried		Air Dried	
		Day 1	Day 128	Day 1	Day 128
Al	$\text{Al}(\text{OH})_3 \text{ aq}$	6	5	1	8
	$\text{Al}(\text{OH})_4^-$	94	95	99	91
Si	H_4SiO_4	98	98	87	99
	H_3SiO_4^-	2	2	13	1
Fe(II)	Fe^{2+}	64	68	60	67
	FeOH^+	1	2	9	1
	$\text{FeSO}_4 \text{ aq}$	35	30	32	31
Fe(III)	FeOH_2^+	29	19	1	39
	$\text{FeOH}_3 \text{ aq}$	29	26	7	29
	FeOH_4^-	42	55	92	32
Ca	Ca^{2+}	62	66	58	66
	$\text{CaSO}_4 \text{ aq}$	38	34	35	34
Mg	Mg^{2+}	65	69	61	69
	$\text{MgSO}_4 \text{ aq}$	35	31	33	31
Na	Na^+	96	97	96	97
	NaSO_4^-	4	3	4	3
K	K^+	94	95	95	95
	KSO_4^-	6	5	5	5
PO_4	HPO_4^{2-}	25	22	12	24
	MgPO_4^-	13	16	46	10
	$\text{MgHPO}_4 \text{ aq}$	38	33	16	38
	$\text{CaHPO}_4 \text{ aq}$	16	18	6	20
	CaPO_4^-	5	9	19	5
SO_4	SO_4^{2-}	63	60	65	60
	$\text{CaSO}_4 \text{ aq}$	14	18	14	18
	$\text{MgSO}_4 \text{ aq}$	23	22	21	22
CO_3	CO_3^-	1	1	6	1
	CaHCO_3^+	3	4	2	4
	$\text{CaCO}_3 \text{ aq}$	2	3	9	2
	HCO_3^-	86	84	68	85
	$\text{MgCO}_3 \text{ aq}$	2	2	11	1
	MgHCO_3^+	6	5	4	6

Dissolved carbonate occurred exclusively as H_2CO_3 in the acidic layer and largely as HCO_3^- in the calcareous sample. Carbonate and bicarbonate complexes accounted for only minor fractions of the total Ca and Mg in the calcareous samples (Table 4.2). Aluminum and Fe(III) occurred primarily in hydrolyzed forms. Soluble phosphate was predicted to occur primarily as the neutral triprotonated species in the acidic sample and distributed among complexes with Ca and Mg in the calcareous sample.

Fe(II) species accounted for most of the total Fe in the acidic sample while Fe(III) was the dominant species in the calcareous sample. The total concentration of all Fe(II) species in the extracts from the acidic samples was in the order of $10^{-2} \text{ mol}\cdot\text{kg}^{-1}$ occurring primarily as the free Fe^{2+} ion in solution (Table 4.1). The total concentration of Fe(III) species in the acidic solution was in the order of $10^{-4} \text{ mol}\cdot\text{kg}^{-1}$ largely as sulfate complexes. The total concentration of Fe(II) species in the extracts from the calcareous samples were less than $10^{-10} \text{ mol}\cdot\text{kg}^{-1}$ and the total concentration of Fe(III) species was in the order of $10^{-6} \text{ mol}\cdot\text{kg}^{-1}$ mostly in the form of hydroxide complexes (Table 4.2). Distributions among Fe(II) and Fe(III) species were similar for both air dried and non-dried pretreatments.

Saturation indices (SI) were calculated for many common primary and secondary minerals found in soils with respect to the composition of the extracted pore waters with time. Values for SI for minerals were calculated using MINTEQ (Brown and Allison 1987) as follows:

$$\text{SI} = \text{Log} (\text{IAP} / K_{\text{sp}}) \quad [4.5]$$

Positive values for SI indicate supersaturation of the solution with respect to the mineral; negative values indicate undersaturation.

Values of SI for most minerals in the air dried and non-dried acidic material were negative indicating that they were not stable (Table 4.3). Both positive and negative SI values were observed for minerals in the calcareous material. Primary minerals, such as the feldspars, magnetite, and tremolite, were stable in the calcareous layer but tended to dissolve in the acidic layer. Previous observations (Chapter 2) indicated that the content of these primary minerals in the acidic layer were reduced relative to the calcareous material.

Table 4.3 Saturation indices for selected primary and secondary minerals calculated with respect to the extracted soil solutions after 128 days of incubation. Values for Log K_{sp} are from the database supplied with MINTEQA (Brown and Allison, 1987).

Mineral	Log K_{sp}	Acidic		Calcareous	
		Non-dried	Air Dried	Non-dried	Air Dried
Al(OH) ₃ (amor.)	10.4	-9.9	-8.5	0.3	0.6
Gibbsite	8.77	-8.3	-6.9	1.9	2.2
Dolomite	-17.0	-27	-25	1.8	0.7
Calcite	-8.48	-14	-13	0.8	0.3
Epsomite	-2.14	-2.2	-2.1	-2.3	-2.3
Gypsum	-4.45	0.3	0.2	0.3	0.3
Goethite	0.50	-2.6	-1.5	6.9	7.0
Hematite	-4.01	-0.1	2.0	19	19
Jarosite	-14.8	-0.8	1.3	4.6	5.7
Natrojarosite	-11.2	-4.7	-2.6	1.3	2.5
Thenardite	-0.18	-7.0	-6.9	-8.5	-8.3
AlOH ₂ SO ₄	-3.23	-0.3	0.3	-4.7	-3.8
α-Quartz	-4.01	1.9	1.8	-0.2	-0.3
SiO ₂ (amor.)	-2.71	0.6	0.5	-1.5	-1.6
Magnetite	3.74	-8.2	-5.3	17	14
Kaolinite	5.53	-8.8	-6.3	7.1	7.7
Muscovite	13.0	-19	-15	11	11
Anorthite	25.4	-29	-26	1.4	1.4
Microcline	0.62	-7.6	-6.1	2.1	1.9
Albite	2.59	-9.8	-8.3	0.3	0.3
Tremolite	56.5	-76	-70	8.3	4.2

Values of SI for jurbanite ($\text{AlOH}\text{SO}_4 \cdot 5\text{H}_2\text{O}$; $\text{Log } K_{\text{sp}} = -3.80$) and gypsum ($\text{CaSO}_4 \cdot 2\text{H}_2\text{O}$; $\text{Log } K_{\text{sp}} = -4.45$) in the acidic sample and gypsum and calcite (CaCO_3 ; $\text{Log } K_{\text{sp}} = -8.48$) in the calcareous sample were plotted against day of extraction to demonstrate the observed trends in mineral solubilities with respect to changes in solution chemistry as influenced by time and drying pretreatment (Figure 4.5). Saturation indices for gypsum were close to zero but slightly positive in both the acidic and calcareous samples (Table 4.3; Figure 4.5). Values for the air dried and non-dried pretreatments were also similar in both the acidified and calcareous samples. In the case of jurbanite in the non-dried acidic sample, SI values were initially negative but increased towards zero with time. Air drying the sample elevated initial total concentrations of Al in solution (Figure 4.3) compared to the non-dried sample and correspondingly increased the SI values for jurbanite close to zero. In the case of calcite in the calcareous sample, SI values were greater than 2.0 at the beginning of incubation but decreased to values close to zero after about 40 days of incubation. SI values for calcite in the non-dried calcareous sample were variable within 0.4 units but remained at values slightly greater than zero during the entire incubation period.

The increases in the concentrations of mineral constituents in the non-dried acidic samples (Figures 4.2 and 4.3) were reflected in increases in the negative SI values for minerals (e.g. jurbanite; Figure 4.5). Undersaturation of the soil solution with respect to jurbanite at the beginning of the incubation period indicated that the activities (and correspondingly the total concentrations) of Al^{3+} and SO_4^{2-} were not high enough to support the formation of the mineral. The low concentrations were likely a reflection of leaching of the acidic layer in the field (Chapter 2). Alternatively, increases in sample temperature from ambient conditions in the field to 25°C may have increased reaction rates and/or shifted the equilibrium values in favour of the solution phase resulting in the observed increase in solution concentrations and mineral dissolution with time. However, large shifts in the thermodynamic equilibrium values due to temperature were not likely as similar changes were not evident in the chemistries of the extracts from the calcareous samples.

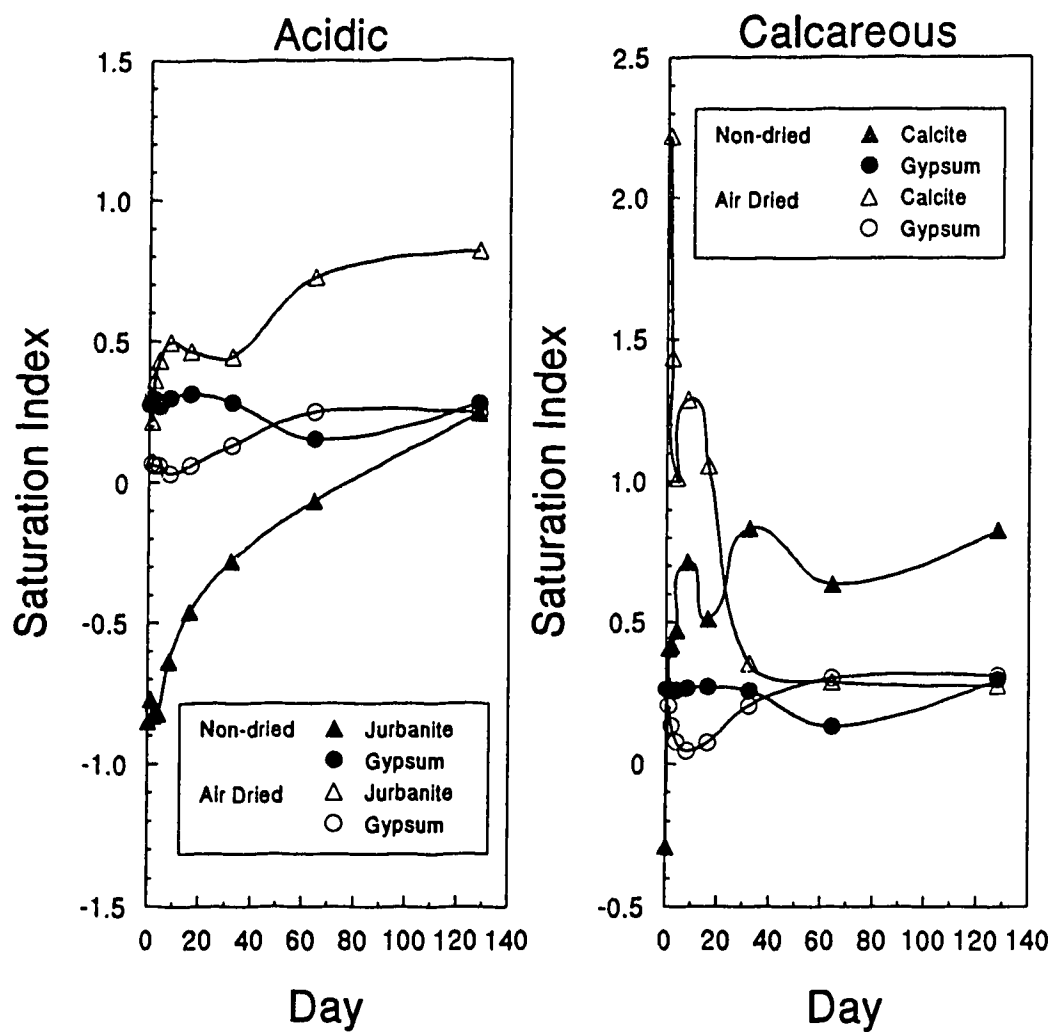


Figure 4.5 Saturation indices for jurbanite and gypsum in the acidic sample and gypsum and calcite in the calcareous sample as plotted against number of days after the start of incubation. Open symbols indicate values for the air dried samples, and closed symbols indicate values for the non-dried samples.

4.4 CONCLUSIONS

The concentration of solutes in the pore water extracts represented the chemistry of the bulk soil solution under conditions of near static temperature, and moisture conditions. The extracted solutions accounted for about 40% of the total mass of solution in the samples at field capacity moisture content (33.3 kPa tension), but the chemistry of the extracts was representative of the bulk soil solution at the time of extraction. Solution was displaced from pores with diameters greater than 0.3 μm . From the initiation of the controlled environmental conditions the concentration of solutes progressed towards steady state levels as controlled primarily by the solubility of soil minerals under the influence of two extremes in soil pH conditions and in the absence of solution flux.

The results of this study demonstrated that the least 15 to 20 days of incubation are required after arrest of temperature and moisture content fluctuations before the concentration of solutes in the soil solution approached stable values. During the initial 15 days of incubation, the chemical composition of the soil solutions extracted from the non-dried samples displayed fluctuations in response to sample handling and arrest of moisture flux. Air drying the samples caused increases in solution pH values for the initial extracts and perturbations in the concentration of solutes requiring, in some cases, up to 60 days of incubation before solute concentrations approached stable values with respect to time.

Extracted solutions from the extremely acidic samples were undersaturated with respect to most common primary and secondary soil minerals. Solute concentrations in the extremely acidic environment increased, sometimes as a linear function of time, until the IAP of a solubility controlling mineral (e.g. jurbanite or gypsum) were approached. The concentration of some solutes in the non-dried acidic samples increased towards, but did not reach, steady state levels even after 128 days of incubation at near constant temperature and moisture content. The concentration of major elements in the extracts from non-dried calcareous samples achieved steady state conditions within 20 days of incubation.

The times required for dissolved solutes to reach steady state concentrations under conditions of static temperature, and moisture content in the current study were ten times longer than the 1 to 2

days reported by others to reach "equilibrium" for re-wet air-dried soil samples or simple mineral systems (Kittrick 1980; Menzies and Bell 1988). Air drying the soil samples for the present study altered solution pH values and produced solute concentrations that changed rapidly during the initial period of the incubation and longer periods of time were required to approach steady state levels compared to samples that were not dried prior to incubation. Increased solute concentrations in extracted pore waters in response to rewetted air dried soils have been reported by others (Qian and Wolt 1990). In the current study the concentration of some solutes were elevated in the extracts of the air dried samples compared to the non-dried samples due to the dissolution of efflorescent salts formed during the air drying pretreatment. Variations in the soluble concentrations of P in the air dried samples were attributed to microbial stimulation on rewetting. Air drying of soil samples may therefore introduce artifacts that result in solute concentrations that are less representative of sample conditions compared to samples that are not dried prior to incubation. The concentration of solutes in the air dried calcareous samples were similar to those of the non-dried samples after about 20 days of incubation. The distribution of species among dissolved components was altered little with changes in the total concentrations of dissolved solutes.

4.5 REFERENCES

- Adams, F., C. Burmester, N.V. Hue, and F.L. Long. 1980. A comparison of column-displacement and centrifuge methods for obtaining soil solutions. *Soil Sci. Soc. Am. J.* 44:733-735.
- Baas-Becking, L.G.M., I.R. Kaplan, and D. Moore. 1960. Limits of the natural environment in terms of pH and oxidation-reduction potentials. *J. Geol.* 68:243-284.
- Beke, G.J. and C.J. Palmer. 1989. Subsurface occurrence of mirabilite in a Mollisol of southern Alberta, Canada: A case study. *Soil Sci. Soc. Am. J.* 53:1611-1614.
- Brown, D.S., and J.D. Allison. 1987. MINTEQA1, An equilibrium metal speciation model: User's Manual. Report No. EPA/600/3-87/012, U.S. Environmental Protection Agency, Athens, GA 92pp.
- Diamond, S. 1970. Pore size distributions in clays. *Clays and Clay Mins.* 18:7-23.
- Dudas, M.J. and S. Pawluk. 1982. Reevaluation of the occurrence of interstratified and other phyllosilicates in southern Alberta soils. *Can. J. Soil Sci.* 62:61-69.
- Edmunds, W.M. and A.H. Bath. 1976. Centrifuge extraction and chemical analysis of interstitial waters. *Environ. Sci. and Tech.* 10:467-472.

- Elkhatib, E.A., O.L. Bennett, V.C. Baligar, and R.J. Wright. 1986. A centrifuge method for obtaining soil solution using an immiscible liquid. *Soil Sci. Soc. Am. J.* 50:297-299.
- Felmy, A.R., D.C. Girvin, and E.A. Jenne. 1984. MINTEQ--A computer program for calculating aqueous geochemical equilibria. Report No. EPA-600/3-84-032, U.S. Environmental Protection Agency, Athens, GA 98pp.
- Furrer, G., J. Westall, and P. Sollins. 1989. The study of soil chemistry through quasi-steady-state models: I. Mathematical definition of model. *Geochim. Cosmochim. Acta.* 53:595-601.
- Gillman, G.P. 1976. A centrifuge method for obtaining soil solution. Div. Soils Rep. no. 16. CSIRO, Australia.
- Hillel, D. 1971. *Soil and water: Physical principles and processes*. Academic Press, NY, p185.
- Kinniburgh, D.G. and D.L. Miles. 1983. Extraction and chemical analysis of interstitial water from soils and rocks. *Environ. Sci. Tech.* 17:362-368.
- Kittrick, J.A. 1980. Gibbsite and kaolinite solubilities by immiscible displacement of equilibrium solutions. *Soil Sci. Soc. Am. J.* 44:139-142.
- Kittrick, J.A. 1983. Accuracy of several immiscible displacement liquids. *Soil Sci. Soc. Am. J.* 47:1045-1047.
- Kodama, H. 1979. Clay minerals in Canadian soils: Their origin, distribution and alteration. *Can. J. Soil Sci.* 59:37-58.
- Longmire, P., D.G. Brookins, and B.M. Thomson. 1990. Hydrogeological interactions and evolution of acidic solutions in soil. pg 154-168. IN D.C. Melchior and R.L. Bassett. Eds. *Chemical modeling in aqueous systems II*. ACS Symp. Series #416. Washington, D.C.
- McKeague, J.A. (ed.) 1978. *Manual on soil sampling and methods of analysis*. 2nd Edition. Can. Soc. Soil Sci. Subcommittee on methods of analysis.
- Menzies, N.W., and L.C. Bell. 1988. Evaluation of the influence of sample preparation and extraction technique on soil solution composition. *Aust. J. Soil Res.* 26:451-464.
- Mubarak, A. and R.A. Olsen. 1976. Immiscible displacement of the soil solution by centrifugation. *Soil Sci. Soc. Am. J.* 40:329-331.
- Pawluk, S. 1961. Mineralogical composition of some grey wooded soils developed from glacial till. *Can. J. Soil Sci.* 41:228-240.
- Peterson, S.R., C.J. Hosteler, W.J. Deutsch, C.E. Cowan. 1987. MINTEQ User's Manual, NUREG/CR-4804, PNL-6106, U.S. Nuclear Regulatory Commission, Washington, D.C. 152pp.
- Qian, P. and J.D. Wolt. 1990. Effects of drying and time of incubation on the composition of displaced soil solution. *Soil Sci.* 149:367-374.
- Rai, D., and J.A. Kittrick. 1989. Mineral equilibria in the soil system. Pages 161-198. IN J.B. Dixon and S.B. Weed eds. *Minerals in soil environments*. 2nd Ed. Soil Sci. Soc Am., Madison, Wisconsin.

- Rhoades, J.D. 1982. Soluble salts. IN A.L. Page, R.H. Miller, and D.R. Keeney. (ed.) Methods of soil analysis. II Chemical and microbiological properties. 2nd Edition. Am. Soc. Agron. Inc., Madison, WI.
- Simard, R.R., L.J. Evans, and T.E. Bates. 1988. The effects of CaCO_3 and P on the soil solution chemistry of a Podzolic soil. *Can. J. Soil Sci.* 68:41-52.
- Sposito, G. 1981. The thermodynamics of soil solutions. Oxford Press, NY. 223pp.
- Whelan, B.R. and N.J. Barrow. 1980. A study of a method for displacing soil solution by centrifuging with an immiscible liquid. *J. Environ. Qual.* 9:315-319.
- Wolt, J. and J.G. Gravel. 1986. A rapid routine method for obtaining soil solution using vacuum displacement. *Soil Sci. Soc. Am. J.* 50:602-605.

5. LAYER CHARGE DENSITY AND CHEMICAL COMPOSITION OF SMECTITE IN A WESTERN CANADIAN SOIL

5.1 INTRODUCTION

Minerals of the clay size fraction of soils from the Interior Plains region of western Canada are commonly reported to be dominated by admixtures of discrete smectite, and clay-sized mica, with lesser amounts of kaolinite, chlorite, and quartz (Rice et al. 1959; Pawluk 1961; Kodama 1979; Dudas and Pawluk 1982; Spiers et al. 1989). These clay minerals are allogenic; derived mainly from underlying Cretaceous sedimentary rocks. The relative proportions of the clay minerals in the $< 2 \mu\text{m}$ size fraction are generally consistent throughout the region.

Although the development of more or less standardized pretreatments and procedures for X-ray diffraction have facilitated qualitative identification and semi-quantification of the clay minerals in soils, details on the chemical characteristics of soil phyllosilicates, most notably smectites, are lacking. Isolation of monomineralic fractions of clay minerals from soils is difficult and confounded because of the complexity and variety of clay minerals found in most soils. Rare occurrences of monomineralic clay mineral fractions comprised completely of smectite have been characterized (e.g. Curtin and Mermut 1985), but the chemical composition may not be representative of smectite found in soils containing mixtures of clay minerals. The physical isolation of pure monomineralic fractions based on particle size separation, most commonly performed by sedimentation (e.g. McKeague 1978; Jackson 1979), is usually not possible because some amount of almost all clay minerals can usually be found within any given size range within the $< 2 \mu\text{m}$ size fraction. The possibility of interstratification of some clay minerals within single particle domains also obstructs separation of monomineralic fractions by sedimentation. Similarly, magnetic separation of iron containing fractions (ferromagnetic and paramagnetic) is also constrained because iron is usually not restricted to one type of clay mineral in a natural mixture (Berry and Jorgensen 1969; Schulze and Dixon 1979).

Problems with the isolation of monomineralic clay fractions hamper studies that involve weathering processes of clays in soil mixtures. As a result, control mechanisms on the stability of minerals, such as smectite, in soil are not well understood. Smectite is usually considered unstable in

acidic environments (Kittrick 1971), yet it is commonly identified in acidic soils (Pawluk 1971; Douglas 1982; Karathanasis and Hajek 1984; Curtin and Mermut 1985). New and innovative approaches are therefore required to characterize clays that occur within soil mixtures and to study their response to changing chemical environments such as acidification.

This chapter reports on an alternative approach used to determine the chemical composition of smectites and other clays. The technique involves determining the total chemical composition of the clay fraction, as well as collecting other chemical and physical data obtained by a variety of analytical techniques, to derive the characteristics and quantify all identifiable minerals in the sample.

The specific objective was to estimate the chemical composition of smectite clay common to soils of the Interior Plains of western Canada using a series of analyses including layer charge density measurements. The technique is also sensitive to differences in the chemical composition of clay minerals and therefore it was used here to identify differences in the chemical compositions of smectites found in acidic and calcareous soil environments.

5.2 MATERIALS AND METHODS

Samples used in this study were collected from beside a 25 year old elemental sulfur block located on the site of a sour gas plant (Chapter 2). The parent surficial material at the site was late-Wisconsin calcareous till of continental origin. The soil surface within three meters of the perimeter of the sulfur block was extremely acidic due to the oxidation of elemental sulfur. The clay sized fraction (<0.002 mm diameter) was dominated by smectite and clay sized octahedral mica with lesser quantities of kaolinite, chlorite and quartz. This suite of clay minerals is typical of soils from the Interior Plains region of western Canada (Kodama 1979; Dudas and Pawluk 1982).

Samples representative of acidified and non-acidified layers previously identified within the profile at the site were collected adjacent to the sulfur block (Chapter 2). Samples from the extremely acidic and non-acidic layers were chosen in an effort to examine the effects of the greatly different pH environments on the soil minerals. Soil samples were collected at five cm depth increments from a series of four replicate pits, spaced five meters apart, located two meters from the west wall of the

sulfur block. At this distance from the side of the block the surficial material was extremely acidic ($\text{pH} < 3.0$) to a depth of 45 cm. The samples displayed pH values of about 2.0 in $0.01 \text{ mol}\cdot\text{dm}^{-3} \text{ CaCl}_2$ and contained copious quantities of precipitated gypsum. The underlying material obtained between 65 and 80 cm depth was calcareous. The latter samples contained an average CaCO_3 equivalent of $100 \text{ g}\cdot\text{kg}^{-1}$ and displayed pH values between 7.3 and 7.6 in $0.01 \text{ mol}\cdot\text{dm}^{-3} \text{ CaCl}_2$.

Samples of the acidified and calcareous materials from selected depths were dispersed in distilled water using ultrasonic vibration (Genrich and Bremner 1972) and the clay size fraction ($< 2 \mu\text{m}$) was obtained by repeated gravity sedimentation (Jackson 1979). Phyllosilicate minerals present in the clay separates were identified from X-ray diffractograms of orientated specimens (Chapter 2). Samples of electrolyte free Ca-saturated specimens were dissolved in HF and HNO_3 (Appendix A) and the digests analyzed for total content of Si, Al, Fe, Mg, K, Ca, Na, Mn, and Ti by inductively coupled plasma atomic emission spectrometry (ICP-AES).

Unit cell formulas for the phyllosilicates were calculated using the computer program CLAYFORM (Bodine 1987). For the calculations it was assumed initially that all structural Fe in the samples occurred in the oxidized (expressed as Fe_2O_3) form (Rozenon and Heller-Kallai 1978). The interlayer charge for the calculated smectite structures were based on oxygen equivalency (Gast 1977; Bodine 1987).

The layer charge density of the 2:1 expandable phyllosilicates in the samples were determined from X-ray diffractograms of n-alkylammonium saturated specimens (Weiss 1963; Ruehlicke and Kohler 1981; Ruehlicke and Niederbude 1985; Hausler and Stanjek 1988; Laird 1987; Laird et al. 1988; 1989). The number of carbon atoms (C_n) in the n-alkylammonium cations range from 6 to 18. The n-alkylammonium saturated clays were prepared through treatment with aqueous solutions of n-alkylamine hydrochlorides synthesized from the reaction of the alkylamines with gaseous HCl (Laird 1987). Oriented specimens of the n-alkylammonium saturated clays were prepared on glass by the paste technique (Theissen and Harward 1962; Laird 1987; Laird et al. 1988).

5.3 RESULTS AND DISCUSSION

5.3.1 Layer Charge Density

The mean layer charge densities for the 2:1 expandable clay minerals in the $< 2 \mu\text{m}$ separates were calculated using the X-ray diffraction data for samples from selected layers within the acid and calcareous clay specimens saturated with n-alkylammonium cations ($C_n = 6$ to 18). X-ray diffractograms for a series of alkylammonium saturated specimens of the clay separates from one of the acidic samples are presented in Figure 5.1. The general appearance of the X-ray diffractograms for the n-alkylammonium saturated clay specimens of the calcareous samples were similar to the acidic samples. All samples displayed broad reflections with low angle peaks ($< 9^\circ 2\theta$ Co $K\alpha$ radiation) indicative of the presence of expandable 2:1 clays containing monolayer or bilayer alkylammonium complexes in the interlayer region (Lagaly and Weiss 1969; Lagaly 1981). The diffractograms also displayed strong sharp reflections with peaks at 0.715 nm, indicative of the presence of kaolinite, and 0.997 nm, indicative of the presence of discrete mica. The mineralogical composition of the $< 2 \mu\text{m}$ fraction was typical of continental glacial parent materials located throughout western Canada (Chapter 2). The X-ray diffractograms for the specimens treated with short chain ($C_n = 6$ to 9) alkylammonium derivatives displayed broad peaks with maxima corresponding to basal spacings of 1.34 to 1.36 nm (Figure 5.1) indicating the presence of 2:1 expandable phyllosilicates containing monolayers of straight chain hydrocarbons in the interlayer region. The space occupied by the flat laying organic ion (A_c) is less than the equivalent area (A_e) allowed for occupation by an interlayer alkylammonium cation (i.e. $A_c < A_e$). The equivalent area (A_e) is defined as (Lagaly and Weiss 1969; Lagaly 1982; Laird et al. 1989):

$$A_e = d(100) \cdot d(010) / 2\sigma \quad [5.1]$$

where $d(100)$ and $d(010)$ are the corresponding unit cell dimensions for the phyllosilicate and σ is the layer charge density. The value for $d(100) \cdot d(010)$ is usually taken as 0.465 nm^2 for smectites (Stul and Mortier 1974; Laird et al. 1989). The equivalent area for the flat laying alkylammonium cation (A_c) is

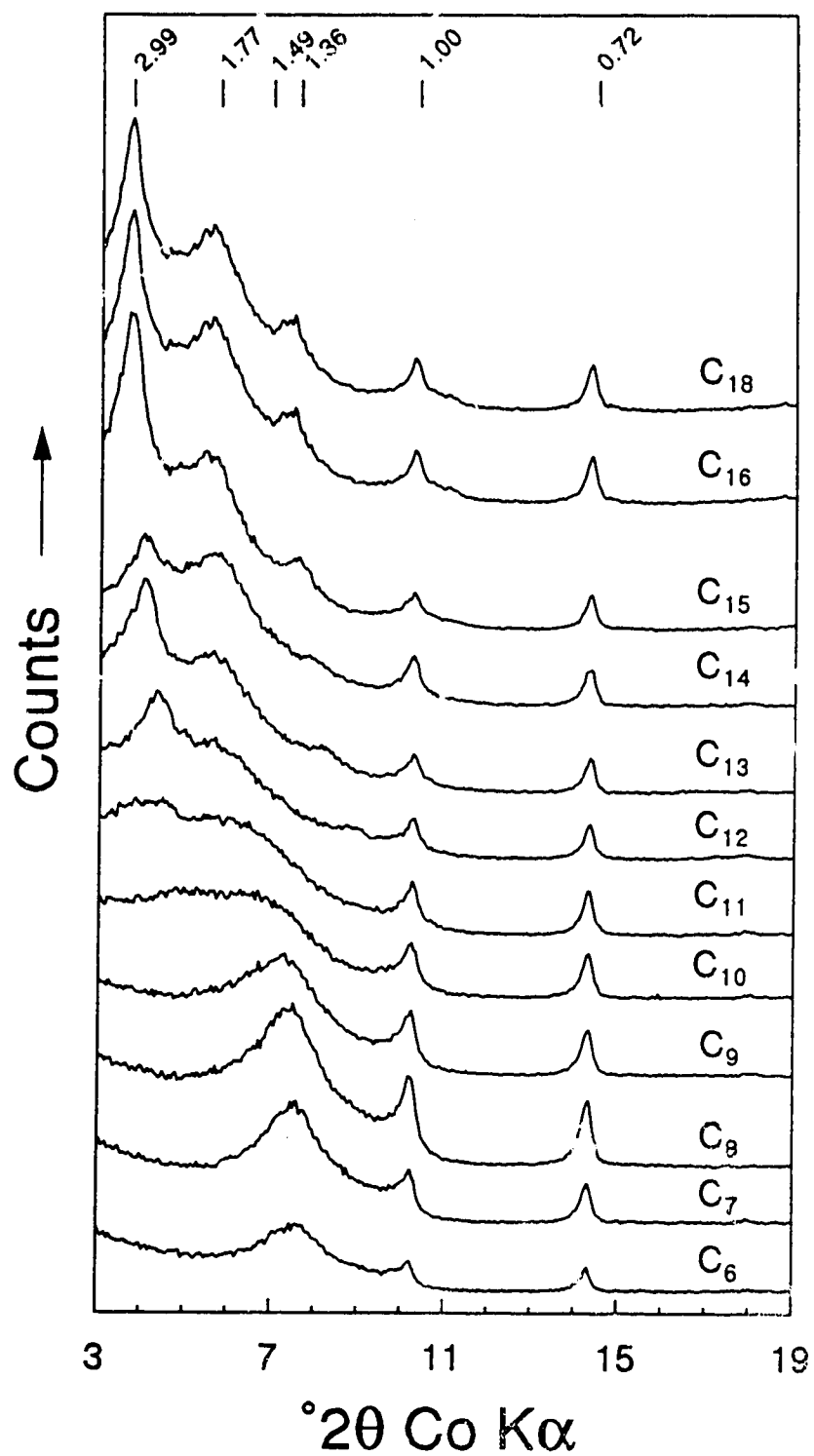


Figure 5.1 X ray diffraction patterns for the alkylammonium saturated clay separates from the acidified material. Values along the top indicate d-spacings in nm.

defined as a function of the number of carbon atoms (C_n) in the straight chain alkylammonium molecule (Lagaly and Wiess 1979; Lagaly 1982; Stul and Mortier 1974):

$$A_c \text{ (nm}^2\text{)} = 0.567C_n + 1.4 \quad [5.2]$$

Diffraction patterns for specimens treated with alkylammonium derivatives containing more than nine carbon atoms ($C_n > 9$) displayed two broad peaks at low angles of 2θ (Figure 5.1). The more diffuse of the two peaks, located at higher angles, corresponded to basal spacings that increased from 1.36 to 1.77 nm for carbon chain lengths of 10 to 14 (Figure 5.2) which indicated the formation of a monolayer-bilayer transition (i.e. $A_c = A_e$). For carbon chains with $C_n > 14$, d-spacings remained at 1.77 nm corresponding to the presence of bilayers in the interlayer region ($A_c < A_e$). The sharper reflections observed at angles less than $5^\circ 2\theta$ (Co K α) in diffraction patterns for $C_n > 9$ (Figure 5.1) displayed maxima that increased linearly from about 2.0 nm for $C_n = 10$ to 2.99 nm for $C_n = 18$ (Figure 5.3). Second order reflections for the more intense low angle peaks were also observed in specimens for $C_n > 11$ (Figure 5.1). The linear increase in the low angle d-spacings with increasing C_n corresponds to the formation of paraffin-like or pseudotrimolecular structures in the interlayer region of the 2:1 expandable clays (Lagaly 1982).

The results obtained for the alkylammonium saturated clays that expanded between 1.36 and 1.77 nm (Figure 5.2) were used to calculate the average layer charge density of the smectite clays in the < 2 μm separates from both the acidic and calcareous samples. Layer charge densities (σ) were calculated as a function of C_n based on an empirically derived mathematical relationship (Laird et al. 1989):

$$\sigma = \frac{38.88}{0.67(C_n) + 14} - 0.078 \quad [5.3]$$

where σ is expressed in units of moles of charge per half cell formula ($\text{mol}(-)/\text{O}_{10}(\text{OH})_2$). The fraction of the total amount of expandable 2:1 clay (p) assigned to each charge density range was calculated

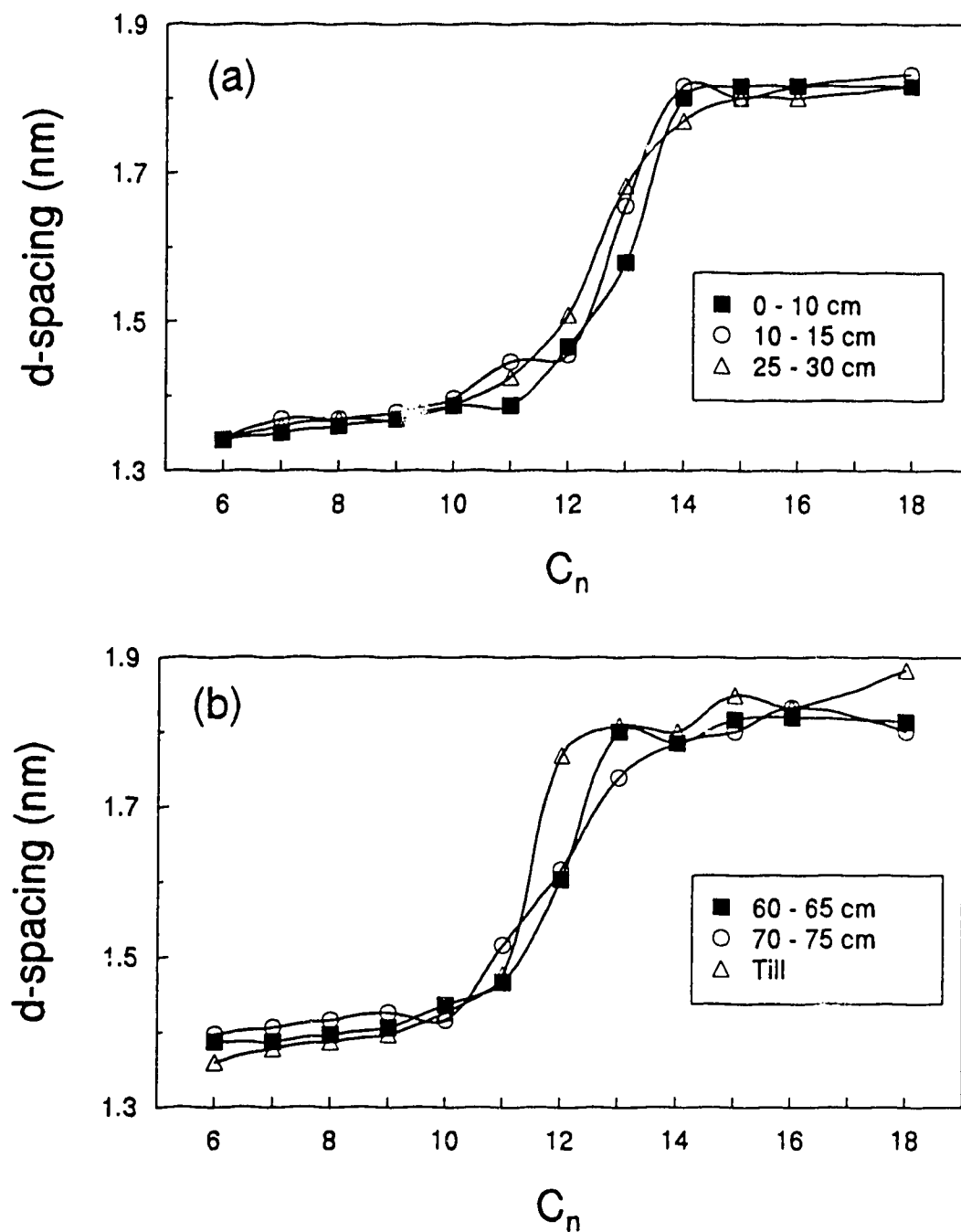


Figure 5.2 Relationship between basal spacing (d-spacing) and length of alkylammonium carbon chain for clay sized separates from the acidified layer (a) and the calcareous layer (b) displaying a monolayer-bilayer transition.

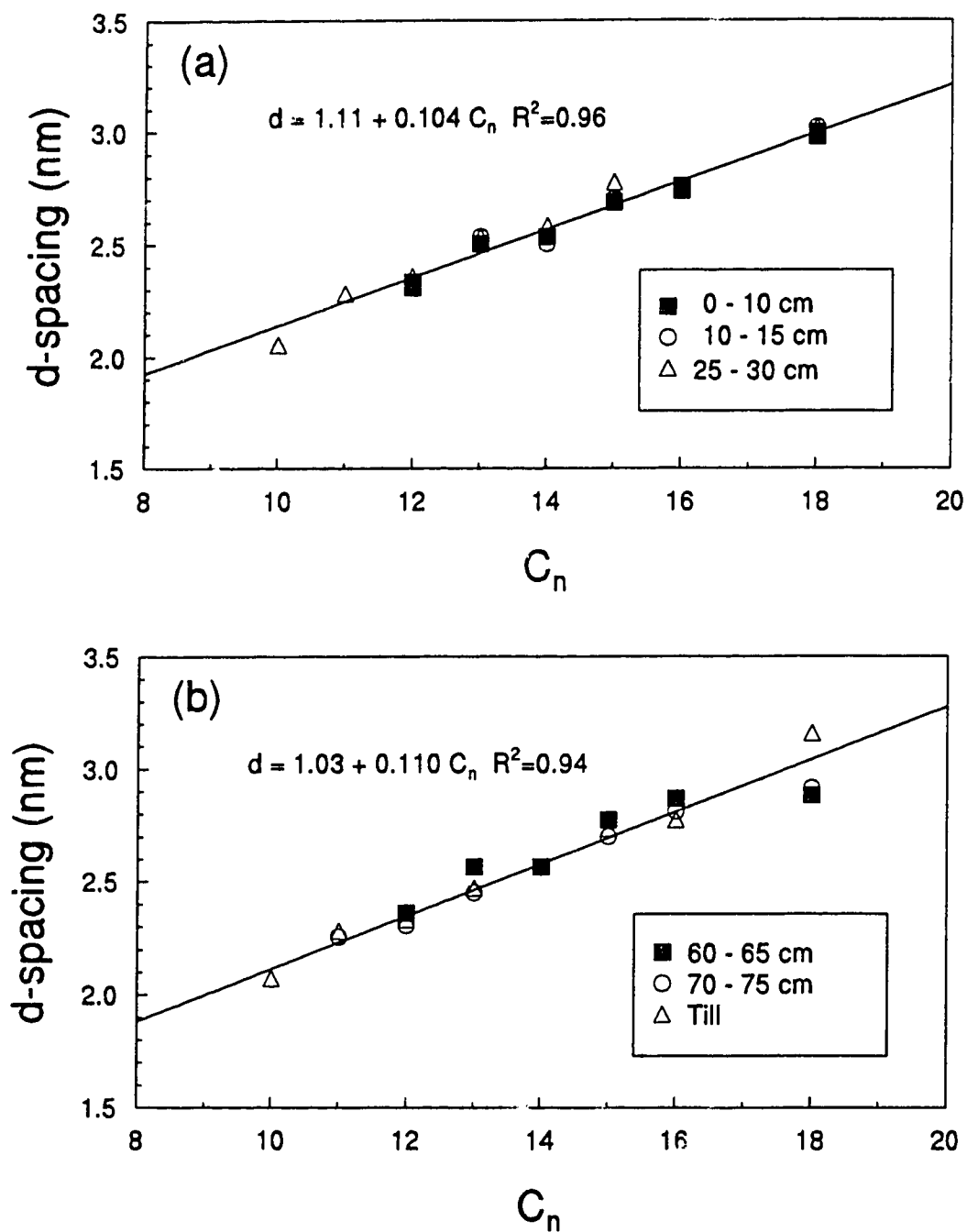


Figure 5.3 Relationship between basal spacing (d-spacing) and length of alkylammonium carbon chain for clay sized separates from the acidified layer (a) and the calcareous layer (b) displaying formation of a paraffin-like structure in the interlayer.

using the following third order polynomial equation:

$$p = -86691 + 16672(d) - 1072.7(d)^2 + 23.203(d)^3 \quad R^2 = 0.9994 \quad [5.4]$$

based on the data presented by Lagaly (1981) for d-spacings (d) between 1.36 and 1.77 nm.

Histograms representing the calculated frequencies for layer charge density ranges for the smectites from the acidic and calcareous samples displayed normal distributions around a mean value (Figure 5.4). Layer charge densities for the smectites from the acidic material (Figure 5.4a) ranged from 0.315 to 0.472 mol(-)/O₁₀(OH)₂ with a mean value of 0.372 mol(-)/O₁₀(OH)₂. The smectites from the calcareous material had σ ranging from 0.338 to 0.580 mol(-)/O₁₀(OH)₂ with a mean value of 0.399 (Figure 5.4b). The reduced σ for smectite from the acidified material compared to the calcareous material indicated that although smectite initially in the calcareous till had not been totally dissolved during acidification at the soil surface (Chapter 2) the smectites had been chemically attacked resulting in a net loss in permanent charge.

The presence of reflections at angles less than 5°2 θ (Co K α) for the alkylammonium saturated clays (Figure 5.1) indicated the presence of 2:1 expandable clay minerals with σ greater than 0.6 mol(-)/O₁₀(OH)₂ which corresponded to the layer charge criterion required to meet the definition for vermiculite (Lagaly 1982; Bailey et al. 1980). The d-spacings values observed at low angles (5°2 θ , Co K α radiation) increased as a linear function of C_n (Figure 5.3). The slope (Δd) of the linear function relating d-spacing to C_n is related to the angle of tilt (α) for the alkylammonium carbon chains interfingered in a paraffin-like structure in the interlayer region of the 2:1 structure as follows (Lagaly and Weiss, 1969):

$$\sin \alpha = \frac{\Delta d}{0.126} \quad [5.5]$$

The value of σ for the phyllosilicate is related to the angle of tilt (α) of the alkylammonium chains in the interlayer and can be calculated using the following regression equation:

$$\sigma = -0.0181 + 189.9(1/\alpha) - 7966(1/\alpha)^2 \quad R^2 = 0.995 \quad [5.6]$$

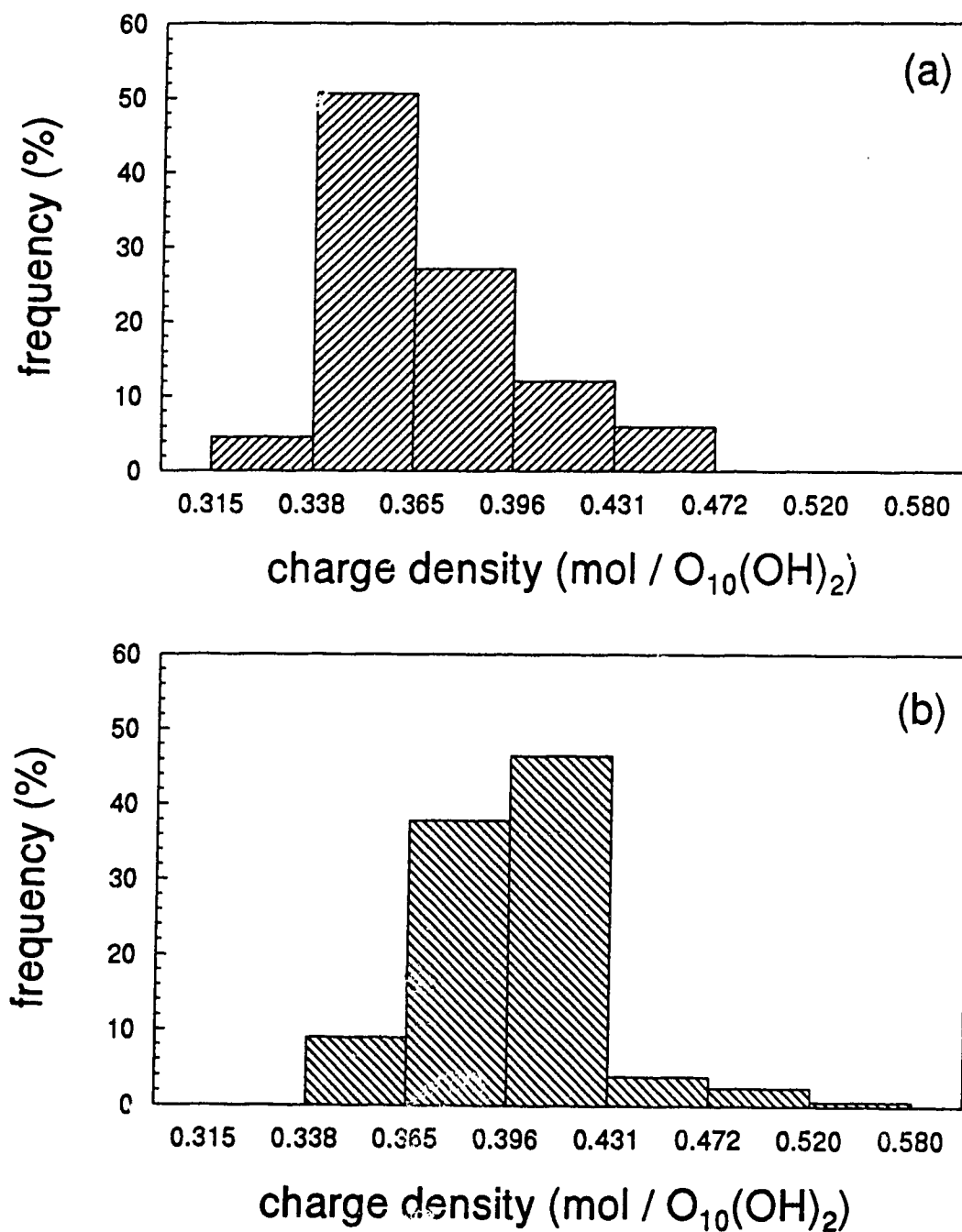


Figure 5.4 Histograms for the distribution of layer charge densities (σ) for smectite from the acidic (a) and calcareous (b) materials.

based on the data of Lagaly (1990). Equations 5.5 and 5.6 were used to calculate the angle of tilt (α) for the n-alkylammonium chains in the interlayer of the vermiculite-like phyllosilicate(s) and the corresponding layer charge density (σ). For the acidic material α was 60.8° which corresponded to a value for σ of $0.78 \text{ mol(-)/O}_{10}(\text{OH})_2$. The equivalent values calculated for the calcareous material were 55.6° and $0.64 \text{ mol(-)/O}_{10}(\text{OH})_2$.

The presence of vermiculite in the samples was not supported by previous observations for the same samples (Chapter 2). X-ray diffraction data and the inability of the clays to fix significant quantities of K indicated the absence of significant quantities of vermiculite in the samples. The detection of vermiculite-like structures in the clay sized fractions by the alkylammonium technique may have been due to the increased sensitivity of the method (Lagaly 1981) enabling detection of very small amounts ($< 5\%$) of vermiculite. The appearance of vermiculite-like structures may have also been an artifact resulting from the removal of interlayer K^+ from clay-sized mica in the sample (Ross and Kodama 1986; Laird et al. 1987). The presence of the second order peaks for $C_n > 11$ suggested that the vermiculite-like structure had few crystalline defects further indicating that the structures were depotassified micas formed during treatment of the samples with the n-alkylammonium compounds.

5.3.2 Chemical Composition

Total chemical composition of the clay separates from the acidic and calcareous horizons are presented in Table 5.1. Silicon and Al were the major components of the clay fraction with lesser amounts of Fe, Mg, Ca, K, Na, Ti and Mn. Acidification reduced the amount of total Al, Fe, Mg, Mn, and Na in the clay fraction. The total contents of K and Ca in the acidified material were not significantly different (Chapter 2) from the calcareous material. Contents of Si and Ti in the acidified material were enriched relative to the calcareous material.

The chemical composition of smectite in the acidified and non-acidified samples was calculated from the bulk clay composition after correcting for the elemental composition of all other minerals in the clay sized fraction (Table 5.1). The structural unit half-cell formula for the smectite (Table 5.2) was subsequently calculated based on oxygen equivalency (Carmichael 1982).

Table 5.1 Mean values for chemical compositions ($\text{g}\cdot\text{kg}^{-1}$) and relative standard deviations (RSD) for the bulk clay and the calculated composition of smectite from the 0 to 10 cm (acidic) depth and the 55 to 75 cm (calcareous) depth.

Component	<u>Bulk Clay</u>				<u>Smectite Composition</u>	
	<u>Acidic</u>		<u>Calcareous</u>		<u>Acidic</u>	<u>Calcareous</u>
	<u>Mean</u>	<u>RSD*</u>	<u>Mean</u>	<u>RSD*</u>		
SiO ₂	656	1.9	568	2.8	610	632
TiO ₂	9.4	4.1	6.1	3.8	25.4	15.1
Al ₂ O ₃	215	4.8	230	2.8	218	217
Fe ₂ O ₃ **	23.6	8.2	66.0	12	20.4	21.4
CaO	11.1	11	10.5	10	30.0	29.8
MgO	12.4	6.6	20.8	2.1	16.1	35.5
MnO	0.1	12	0.2	58	0.1	0.4
K ₂ O	32.1	3.3	29.2	4.9	0.0	0.0
Na ₂ O	4.6	14	6.1	13	12.4	4.6
LOI ***	64.7	12	63.8	20	93.5	63.1
Total	1030		990		1030	1020

* Expressed as percent (%)

** Total Fe expressed as Fe₂O₃.

*** LOI = Loss on Ignition at 850°C.

Table 5.2 Unit half-cell formulas and quantities ($\text{g}\cdot\text{kg}^{-1}$) of minerals and amorphous phases in the < 2 μm size fraction separated from the acidic and calcareous layers.

<u>Mineral</u>	<u>Unit Cell Half Formula</u>	<u>Fraction of Total</u>	
		<u>Acidic</u>	<u>Calcareous</u>
Kaolinite	$\text{Al}_4\text{Si}_4\text{O}_5(\text{OH})_4$	111	119
Mica	$\text{K}_{0.85}[\text{Si}_{3.35}\text{Al}_{0.65}][\text{Al}_{1.55}\text{Fe}^{3+}_{0.25}\text{Mg}_{0.10}]\text{O}_{10}(\text{OH})_2$	321	292
Chlorite	$[\text{Si}_{2.59}\text{Al}_{1.41}][\text{Al}_{1.30}\text{Fe}^{2+}_{4.32}\text{Mg}_{0.13}]\text{O}_{10}(\text{OH})_8$	0	65
Fe_2O_3 (am)	Acid ammonium oxalate extractable Fe_2O_3	0	9
SiO_2	Quartz + amorphous SiO_2	196	95
Smectite	$\text{M}^{+}_{0.34}[\text{Si}_{3.98}\text{Al}_{0.02}][\text{Al}_{1.66}\text{Fe}^{3+}_{0.10}\text{Mg}_{0.16}]\text{O}_{9.92}(\text{OH})_{2.08}$	372	-
Smectite	$\text{M}^{+}_{0.40}[\text{Si}_{3.96}\text{Al}_{0.04}][\text{Al}_{1.56}\text{Fe}^{3+}_{0.10}\text{Mg}_{0.33}]\text{O}_{10}(\text{OH})_2$	-	420

Kaolinite identified in the clay fraction was assumed to be of uniform crystallinity and composition (Chittleborough and Walker 1988) and was quantified based on area under the (001) reflections in the X-ray diffraction patterns for the oriented Ca-saturated specimens (Chapter 2). Kaolinite accounted for $111 \text{ g}\cdot\text{kg}^{-1}$ of the total clay in the acidic sample and $119 \text{ g}\cdot\text{kg}^{-1}$ in the calcareous sample (Table 2.5)

The clay-sized mica in the sample was dioctahedral (Chapter 2) and assumed to be derived primarily from plutonic micas of the Canadian shield (Kodama 1979; Miller et al. 1981). The quantities and composition of the clay-sized mica was based on a total content of $100 \text{ g}\cdot\text{kg}^{-1} \text{ K}_2\text{O}$ (Mehra and Jackson 1959). It was assumed that mica accounted for all of the K in the clay sized fractions. The proportional contents of Fe_2O_3 and MgO in the clay sized mica were based on mean values for documented samples (Deer et al. 1966; Routson and Kittrick 1971; Weaver and Pollard 1975).

Chlorite was detected only in the calcareous sample (Chapter 2) and its composition was based on X-ray diffraction data for the oriented K-saturated specimens. The mean d-spacing values for

chlorite in the calcareous till material was 1.414 nm (+/- 0.003) based on the peak positions of the d(003) and d(004) reflections. Content of total Al, Al in tetrahedral coordination (Al^{IV}), and, by difference, Al in octahedral coordination (Al^{VI}) in the chlorite were calculated using the equations of Bailey (1972):

$$d(001) = 1.455 - 0.029(\text{Al}^{\text{IV}}) \quad [5.7]$$

$$d(001) = 1.452 - 0.014(\text{Al}^{\text{IV}} + \text{Al}^{\text{VI}} + \text{Cr}) \quad [5.8]$$

where: d(001) is the basal spacing for chlorite measured in nm. The contribution of Cr to the peak positions for the chlorite was assumed to be negligible. The total amount of Mg in the chlorite was derived from the relationship (Foster 1962, cited by Bailey 1988):

$$\text{Si}^{4+}(\text{IV}) + \text{Mg}^{2+}(\text{VI}) = \text{Al}^{3+}(\text{IV}) + \text{Al}^{3+}(\text{VI}) \quad [5.9]$$

The remaining component of the chlorite was assumed to be Fe_2O_3 . Most chlorites found in soil are trioctahedral and inherited from the parent material (Bailey 1988). The mean octahedral cation site occupation for natural trioctahedral chlorites was taken as 5.75 (range = 5.45 - 6.05; Foster 1962, cited by Neveling and Brown 1987). Chlorite was present in the calcareous layer and absent in the acidic layer (Table 5.2). The differences in the total amounts of Fe_2O_3 and MgO between the acidic and calcareous samples, after accounting for clay-sized mica and acid ammonium oxalate extractable fractions, were therefore allocated to chlorite. The calculated content of chlorite in the clay fraction of the calcareous layer was 65 $\text{g}\cdot\text{kg}^{-1}$. The calculated composition of the chlorite in the calcareous sample indicated that it was Fe rich (Table 5.2), which is consistent with observations for chlorite in other Alberta soils (Pawluk and Lindsay 1964; Spiers 1982). The calculated content of total Fe in the chlorite was greater than 40 $\text{g}\cdot\text{kg}^{-1}$ exceeding the requirements for classification as a ferrous chlorite (Bailey 1988).

The total amount of MnO and TiO₂ in the clay fractions were minor (Table 5.1) and the concentration of all other elements accounted for less than 1 g·kg⁻¹ (0.1%) of the total clay fraction. Much of the TiO₂ in the samples was attributed to the presence of resistant minerals such as rutile in the clay sized fraction. It was assumed that the total quantities of Mn, Ti, and all other minor and trace elements did not significantly affect the calculated composition for the smectite and were therefore excluded from the calculations for the unit cell formulas.

After accounting for the quantities and compositions of the above mentioned minerals, the remaining fraction of the bulk composition was very rich in SiO₂. Preliminary calculations for the unit cell formula of smectite, that included the high content of SiO₂, indicated that the amount of Si present was far in excess of the requirements to fill all tetrahedral sites in an ideal dioctahedral smectite structure. The calculated amount of SiO₂ in the samples allocated to smectite was therefore reduced such that the total contents of Al, Fe, and Mg were correspondingly increased until the requirements for an ideal dioctahedral structure 2:1 phyllosilicate structure were met. The excess SiO₂ was assumed to be present in the form of clay-sized quartz and amorphous SiO₂. The acidic and calcareous samples were accordingly reduced in SiO₂ by 196 and 95 g·kg⁻¹, respectively (Table 5.2). The higher amount of quartz calculated for the acidic sample compared to the calcareous sample were consistent with the relative intensities of the 0.426 and 0.334 nm peaks for α-quartz relative to the intensities of the peaks for the phyllosilicates observed in the clay separates from the acidic and calcareous samples (Figure 2.2). The higher content of quartz in the acidic sample was attributed to enrichment resulting from the dissolution of other minerals (Chapter 2).

The resultant calculated chemical formulas for the smectites in the acidic and calcareous samples (Table 5.2) indicated that the 2:1 expandable clays were characteristic of montmorillonite. The formulas calculated for the smectite indicated very little tetrahedral substitution of Al for Si with almost all permanent charge sites originating within the octahedral sheet. The calculated compositions for the clays from the acidic and calcareous materials were also very similar except for reduction in the amount of Mg in the smectite from the acidic material. Reduction in the total amount of structural Mg, relative